THE SILESIAN UNIVERSITY OF TECHNOLOGY

FACULTY OF CHEMISTRY

DEPARTMENT OF ORGANIC CHEMISTRY, BIOORGANIC CHEMISTRY AND BIOTECHNOLOGY

Anna Blacha, MSc Eng

Chemical Sciences

PhD Thesis

CARBON NANOTUBES AND GRAPHENE AT THE INTERFACE AND IN THE 3D-NETWORK: PHYSICOCHEMICAL MODIFICATIONS FOR FUNCTIONAL SYSTEMS

Nanorurki węglowe i grafen na granicy faz oraz w sieci trójwymiarowej: modyfikacje fizykochemiczne dla układów funkcjonalnych

Supervisor: Prof. Sławomir Boncel, DSc PhD Eng

GLIWICE 2025

ACKNOWLEDGEMENTS

I want to express my heartfelt thanks to my supervisor, **Professor Sławomir Boncel, DSc, PhD, Eng,** for his invaluable assistance, inspiring discussions, patience, and support at every stage of my scientific career. His commitment and openness to new ideas were a constant source of motivation and inspiration for me.

I would like to express my sincere gratitude to **Dr Karolina Milowska, Prof. Krzysztof Kozioł and Prof. Artur Terzyk** for their long-standing collaboration, insightful discussions, and invaluable support.

I would like to thank **Prof. Grzegorz Dzido, Prof. Noorhana Yahya, Prof. Mike C. Payne, Dr Anna Kolanowska, Dr Rafał Jędrysiak, Dr Bertrand Jóźwiak, Dr Roman Turczyn, Dr Juliette Beunat, Dr Emil Korczeniewski, Dr Monika Zięba, Dr Wojciech Zięba, Dr Aleksandra Cyganiuk, Dr Vijay Kumar Thakur, Dr Heather Greer** and **Dr Pak-Lee Chau** for the fruitful cooperation.

I would like to warmly thank all past and current members of the **Nanocarbon Group** for their continuous help and the great atmosphere in our lab. Their enthusiasm, teamwork, and kindness made the years of research an inspiring and memorable experience.

Last but not least, I am deeply grateful to my **Husband, Son and Parents** for their unwavering support, encouragement, And belief in me throughout my doctoral studies. To my family, with love and gratitude — I dedicate this work.

The PhD thesis was financed by the National Science Centre (Poland) Grant No. 2019/33/B/ST5/01412 in the framework of the OPUS program.

TABLE OF CONTENTS

ABSTRACT

Graphene and carbon nanotubes (CNTs) are among the most promising nanomaterials due to their exceptional mechanical strength, electrical and thermal conductivity. However, their effective implementation in macroscale systems remains challenging due to poor dispersibility, incompatibility with polar media, and difficulties with scalable processing. Overcoming these limitations is essential to bridge the gap between the remarkable intrinsic properties of these nanomaterials and their practical applications.

This dissertation is a study of the design of functional graphene- and CNT-based composites, with an emphasis on sustainable, scalable processing methods. The main objectives included understanding the amphiphilic properties of graphene and CNTs to enable the stabilisation of Pickering emulsions, as well as investigating the influence of CNT morphology, including aspect ratio and crystallinity, on the thermophysical performance of paraffin-based nanocomposites and developing a biomimetic approach for graphene modification to achieve stable aqueous dispersions and electroconductive coatings.

Overall, the research provides new insights into how morphology, surface chemistry, and interfacial interactions govern the macroscopic properties of carbon nanostructure-based systems. The development of sustainable routes and multifunctional composites paves the way for scalable, environmentally responsible applications of graphene and CNTs in modern technologies.

ABSTRAKT

Grafen i nanorurki węglowe należą do najbardziej obiecujących nanomateriałów ze względu na ich wyjątkową wytrzymałość mechaniczną oraz przewodność elektryczną i cieplną. Jednak ich skuteczne wdrożenie w systemach makroskopowych pozostaje wyzwaniem ze względu na słabą dyspergowalność, niekompatybilność z mediami polarnymi oraz trudności w skalowalnym przetwarzaniu. Pokonanie tych ograniczeń jest niezbędne, aby wypełnić lukę między niezwykłymi właściwościami tych nanomateriałów a ich praktycznymi zastosowaniami.

Niniejsza rozprawa doktorska jest studium poświęconym projektowaniu funkcjonalnych kompozytów zawierających grafen i nanorurki węglowe, z naciskiem na zrównoważone i skalowalne metody przetwarzania. Główne cele obejmowały zrozumienie właściwości amfifilowych grafenu i nanorurek węglowych w celu umożliwienia stabilizacji emulsji Pickeringa; zbadanie wpływu morfologii nanorurek węglowych, w tym współczynnika kształtu oraz krystaliczności, na właściwości termofizyczne parafinowych nanokompozytów, w niniejszej pracy została również zaproponowana łagodna modyfikacja grafenu w celu uzyskania stabilnych dyspersji wodnych i powłok elektroprzewodzących.

Badania dostarczają nowych informacji na temat tego, w jaki sposób morfologia, chemia powierzchni i oddziaływania międzyfazowe wpływają na właściwości makroskopowe systemów zawierających nanostruktury węglowe. Opracowane zrównoważone metody i wielofunkcyjne kompozyty otwierają drogę do skalowalnych, przyjaznych dla środowiska metod przetwarzania grafenu i nanorurek węglowych dla nowoczesnych technologii.

GLOSSARY

AR	Aspect ratio
AFM	Atomic force microscopy
CNT(s)	Carbon nanotube(s)
CVD	Chemical vapour deposition
DMF	*N,N*-dimethylformamide
EMI	Electromagnetic interference
FBCVD	Fluidised bed chemical vapours deposition
FLG	Few–layered graphene
GNR	Graphene nanoribbon
GO	Graphene oxide
HRTEM	High–resolution transmission microscopy
MLG	Multi–layered graphene
MWCNT(s)	Multi–walled carbon nanotube(s)
NMP	*N*-methylpyrrolidone
RDF(s)	Radial distribution function(s)
rGO	Reduced graphene oxide
SEM	Scanning electron microscopy
SLG	Single–layer graphene
SWCNT(s)	Single–walled carbon nanotube(s)
PCM(s)	Phase–change material(s)
RAM(s)	Radar absorbing material(s)
WCA	Water-contact angle

LIST OF MONOTHEMATIC PUBLICATIONS

[P1] Kuziel A. W.; , Milowska*, K. Z.; Chau, P.; Boncel, S.; Koziol*, K. K.; Yahya, N.; Payne, M. C.; The true amphipathic nature of graphene flakes: a versatile 2D stabilizer, *Advanced Materials* **2020**, *32*, 2000608; https://doi.org/10.1002/adma.202000608.

IF_{2024}=26.8, Ministerial points=200

[P2] Blacha, A. W.; Milowska*, K. Z.; Payne, M. C.; Greer, H. F.; Terzyk, A. P.; Korczeniewski, E.; Cyganiuk, A.; Boncel*, S. The Origin of Amphipathic Nature of Short and Thin Pristine Carbon Nanotubes — Fully Recyclable 1D Water-in-Oil Emulsion Stabilizers, *Advanced Materials Interfaces* **2023**, *10*, 2202407; https://doi.org/10.1002/admi.202202407.

IF_{2024}=4.4, Ministerial points=100

[P3] Kuziel, A. W.; Dzido, G.; Turczyn, R.; Jędrysiak, R. G.; Kolanowska, A.; Tracz, A.; Zięba, W.; Cyganiuk, A.; Terzyk, A. P.; Boncel*; S. Ultra-long carbon nanotube-paraffin composites of record thermal conductivity and high phase change enthalpy among paraffin-based heat storage materials, *Journal of Energy Storage* **2021**, *36*, 102396; https://doi.org/10.1016/j.est.2021.102396.

IF_{2024}=9.8, Ministerial points=100

[P4] Blacha, A.; Dzido, G.; Jędrysiak, R.; Kolanowska, A.; Jóźwiak, B.; Beunat, J.; Korczeniewski, E.; Zięba, M.; Terzyk, A. P.; Yahya, N.; Thakur, V. K.; Kozioł*, K. K.; Boncel*, S. Biomimetically inspired highly homogeneous hydrophilization of graphene with poly(L-DOPA): toward electroconductive coatings from water-processable paints, *ACS Sustainable Chemistry Engineering* **2022,** *10*(20), 6596–6608; https://doi.org/10.1021/acssuschemeng.2c00226.

IF_{2024}=7.3, Ministerial points=140

Wydział Chemiczny
Katedra Chemii Organicznej,
Bioorganicznej i Biotechnologii

mgr inż.
Anna Blacha

doktorant

Gliwice, 12.10.2025 r.

Oświadczenie potwierdzające zmianę nazwiska

Niniejszym oświadczam, że zmianie uległo moje nazwisko

z

KUZIEL.....

(poprzednio używane nazwisko)

na

BLACHA.....

(aktualne nazwisko)

Oświadczam, że ponoszę odpowiedzialność prawną w przypadku podania danych niezgodnych z prawdą.

Z poważaniem,

Blacha Anna

Politechnika Śląska
Wydział Chemiczny
Katedra Chemii Organicznej, Bioorganicznej
i Biotechnologii
ul. Krzywoustego 4, pok. Ł1 , 44-100 Gliwice
anna.blacha@polsl.pl

1. INTRODUCTION

As science and industry enter a new era, true innovation must be centred on sustainability, energy efficiency, and recycling. Global initiatives like the 2030 Agenda, as well as European circular-economy goals, define policies that shift the emphasis away from linear production toward engineering materials for longer lifespans, reuse, and resource recovery.[1]

The world community must shift toward recyclable, waste-free, environmentally friendly materials with low ecological impact to meet this rapidly growing challenge. This approach requires a 'cradle-to-grave' strategy that incorporates 'green chemistry' principles into both the raw material selection and the entire processing path.[2] According to this paradigm, **improved functionality** entails not only improved technical characteristics but also improved circularity, decreased toxicity, and lower energy use.

Nanomaterials, owing to their extraordinary physicochemical properties, represent one of the most promising pathways to meet the growing demand for functional, application-tailored materials.[3] Even a small amount of nanoadditives can significantly increase the strength, hardness, elasticity and durability of a material, allowing components with better performance parameters to be created with less raw material consumption.

Among the wide spectrum of nanomaterials, graphene and carbon nanotubes (CNTs) stand out as the most promising, multifunctional nanomaterials. Their exceptional mechanical, electrical, or thermal properties, tunable morphology, and high surface-to-volume ratio offer options far beyond those of traditional bulk materials. They are therefore desirable candidates for cutting-edge technologies spanning biological and electronic applications, energy conversion and storage, environmental cleanup, and catalysis.[4]

However, there are still significant obstacles to be addressed despite this enormous potential. In addition to leveraging their extraordinary qualities, ongoing research aims to responsibly develop nanomaterials in line with the principles of the circular economy and green chemistry.

1.1. Carbon nanotubes and graphene

CNTs are *quasi*-one-dimensional nanoparticles consisting of cylindrical nanostructures made entirely of carbon atoms organised in a hexagonal lattice, like a rolled-up sheet of graphene. Strong sp^2-hybridised covalent bonds hold the carbon atoms in CNTs, giving them exceptional mechanical strength and stability. These structures have diameters typically in the nanoscale range and lengths ranging from a few micrometres to several millimetres or even centimetres.[5] The global recognition of CNTs is attributed to Sumio Iijima, who in 1991 reported detailed high-resolution transmission electron microscopy (HRTEM) images and a comprehensive structural analysis of multi-walled carbon nanotubes (MWCNTs), igniting worldwide scientific interest in these nanomaterials.[6]

Depending on the number of concentric walls, CNTs can be divided into different groups. A single graphene sheet that has been smoothly rolled into a cylindrical shape, usually with a diameter of 0.4 to 2 nm, forms single-walled carbon nanotubes (SWCNTs). MWCNTs, on the other hand, are made up of several concentric cylinders.[7]

The chiral vector (C_n), which joins two crystallographically identical sites on a graphene sheet, is frequently used to characterise the geometric structure of CNTs (**Fig. 1**). In this expression, **n** and **m** are integers, while $\mathbf{a_1}$ and $\mathbf{a_2}$ are the unit vectors of the hexagonal honeycomb lattice. The number pair (n,m), which defines a CNT's symmetry and classifies it into configurations like armchair (n,n) or zigzag (n,0), and chiral if **n** differs from **m**, determines the topology of the CNT in its entirety.[8]

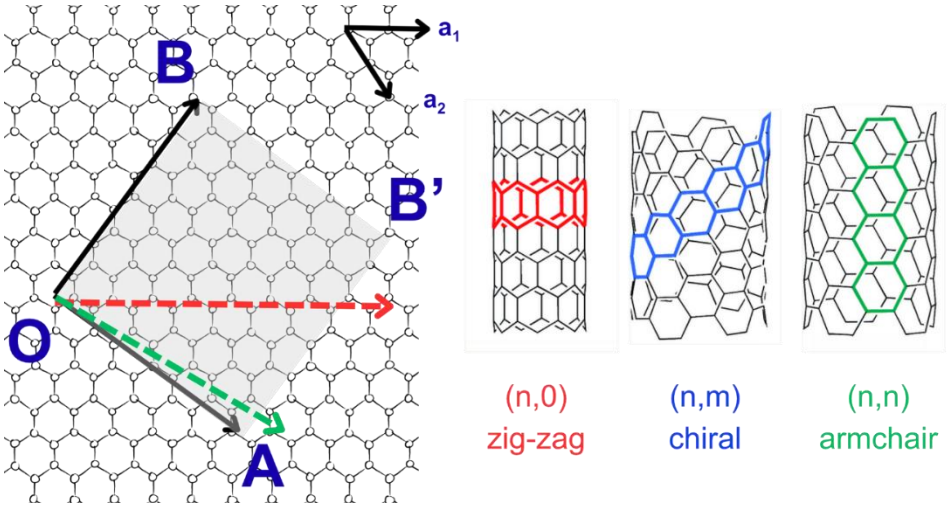

Fig. 1 Chirality vector and types of CNTs.

Actually, vacancies, dislocations, Stone–Wales defects (rotated carbon bonds that form pentagon-heptagon pairs), and occasionally foreign atoms integrated into the lattice are among the structural imperfections that CNTs frequently have (**Fig. 2**).[9] The electrical, mechanical, and chemical characteristics of CNTs can all be strongly impacted by these defects.[10] These defects may weaken tensile strength and Young's modulus, because they break the network of sp^2 bonds;[11] however, they may allow plastic deformation before fracture, yielding an increase in ductility.[12] They also may scatter electrons and phonons, resulting in a decrease in charge mobility.[13]

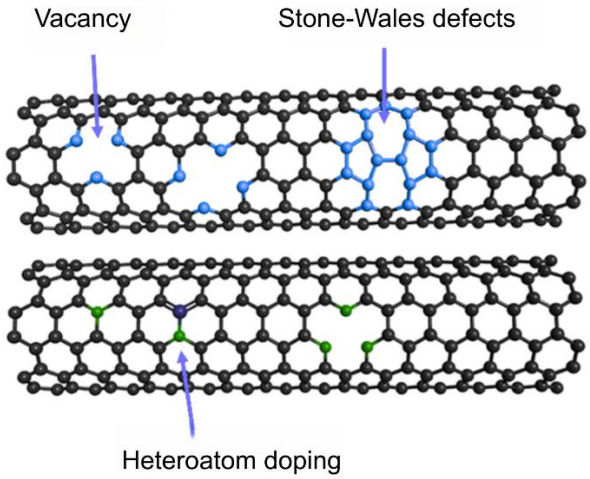

Fig. 2 Defect types in CNTs.[14]

Defects in CNTs may arise during synthesis due to improper temperature conditions or catalyst impurities.[15] The carbon feedstock may not decompose completely when the temperature is too low, resulting in incomplete graphitisation or amorphous carbon deposits.[16] On the other hand, too high a temperature causes catalyst coarsening, resulting in discontinuous growth, vacancies, or open-ended nanotubes.[17,18] In addition, they can also be introduced during post-synthetic treatments, such as surface functionalization,[19] oxidation,[20] or ultrasonic dispersion.[21] Covalent functionalisation of CNT, like chlorination,[22] fluorination,[23] coupling using diazonium salts with the subsequent elimination of nitrogen molecules[24] or oxidation[20] and amination,[25] typically involves attaching the functional groups, which requires breaking of C-C within CNTs structure. These generate vacancies, sp^3-hybridised sites, or disrupted π-conjugation within the sp^2 carbon network. Similarly, oxidation leads to etching, shortening and hole formation.[26] Ultrasounds, which are frequently used for the deagglomeration of CNTs, subject CNTs to high local shear forces and cavitation, which results in bending, scission and defect formation.[27]

Another remarkable nanocarbon allotrope is **graphene**, for which it took six decades to go from early, contentious theoretical predictions to effective experimental isolation. The breakthrough occurred in 2004, when Geim and colleagues successfully isolated a stable monolayer of graphene through mechanical exfoliation. For this pioneering work, Geim and Novoselov received the 2010 Nobel Prize in Physics. Since then, graphene has become one of the most intensively studied 2D materials worldwide.

Graphene is a 2D material, at the atomic scale arranged in a hexagonal lattice, where each vertex is occupied by a single carbon atom exhibiting sp^2 hybridisation, where the carbon-carbon bond length in this configuration is 0.142 nm.[28] A strong hexagonal structure is produced by the three σ bonds that each carbon atom makes inside the plane. The π-bonds, which are aligned perpendicular to the lattice plane, are the main source of the remarkable electrical

conductivity of graphene.[29] According to ISO/TS 80004-13:2017 standard, there are several variants of graphene, which vary primarily in shape, chemical modification, structural quality, and number of layers.[30] **Fig. 3** displays the primary varieties of graphene. One atomic layer of carbon atoms organised in a perfect hexagonal lattice makes up the first category, known as pristine single-layer graphene (SLG).[31] This is the purest form with the highest mechanical strength (Young's modulus ~1 TPa, tensile strength ~130 GPa),[32] optical transparency (~97.7 %),[33] and electrical conductivity of any form of graphene (10^6 $S \cdot m^{-1}$).[34] The second category is few-layer graphene (FLG), made up of 2-10 graphene layers stacked together and held by weak van der Waals forces.[35] The third category is multi-layer graphene (MLG) in the form of graphene nanosheets, which consists of up to 15-30 layers. Beyond this range, the material acts less like isolated graphene sheets and more like thin graphite.[36] Additional examples are graphene nanoribbons (GNRs), which are thin graphene strips having distinct edge patterns like zigzag or armchair that are usually less than 50 nanometers wide.[37] Very often in the literature, one can find studies regarding graphene oxide (GO) or reduced graphene oxide (rGO); however, these forms of graphene differ fundamentally from pristine graphene and, strictly speaking, are not considered as 'true' graphene. GO is heavily decorated with oxygen-containing functional groups, such as hydroxyl, epoxy, and carboxyl groups, which disrupt sp^2 hybridisation and break the continuity of the π-electron system.[38]. In contrast, rGO is obtained by partially removing these oxygen functionalities from GO through chemical, thermal, or electrochemical reduction.[39] Even though rGO retains some of the sp^2 network and electrical conductivity, it still contains residual oxygen groups and structural defects that hinder it from reaching the electrical performance and structural perfection of pristine graphene.

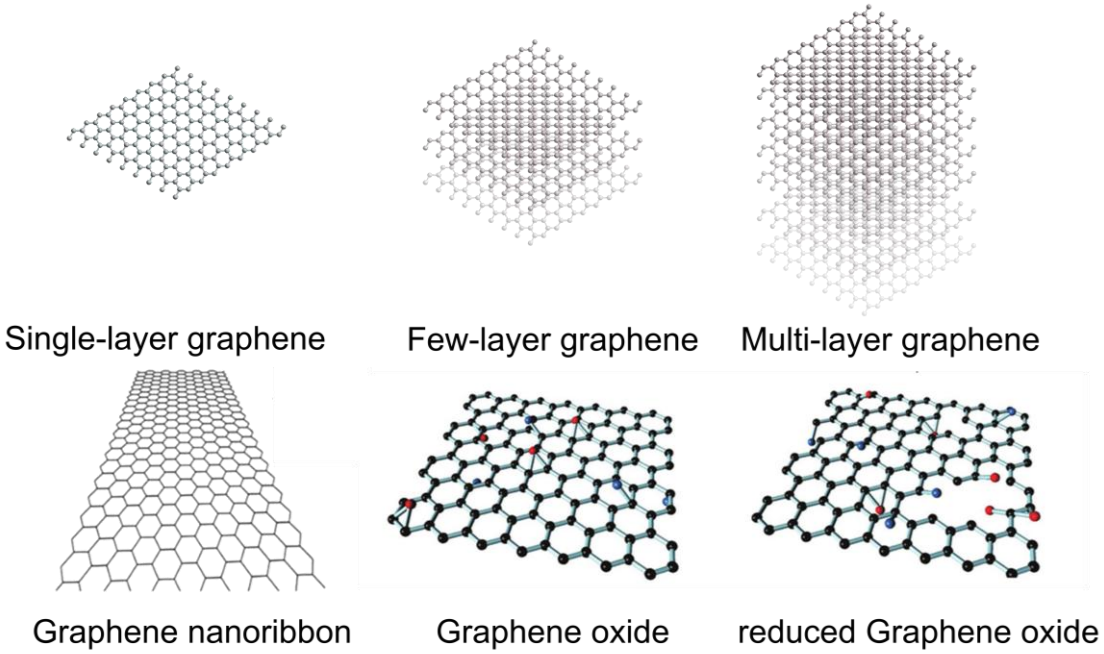

Fig. 3 Structural variants of graphene and its analogues.

Generally, production methods in nanomaterials science are typically divided into two basic categories: top-down and bottom-up approaches. The bottom-up method builds structures from their smallest constituents, such as atoms, ions, or molecules, which are then assembled *via* chemical or physical processes to form larger, more distinct structures. The structure, morphology, and characteristics of the final material can be precisely tailored during this process, which often enables the production of high-quality, low-defect products.[40] Chemical vapour deposition (CVD),[41] arc discharge,[42] laser ablation,[43] and, particularly for graphene, epitaxial growth on specific substrates like SiC[44] are standard bottom-up techniques for carbon nanomaterials. In contrast, the top-down method starts with bulk material and uses lithographic, chemical, or mechanical methods to break it down into nanoscale structures gradually. Although this approach is usually faster and more scalable, the material may acquire defects and irregularities.[45] Mechanical exfoliation (the Scotch tape method),[46] liquid-phase exfoliation,[47] ball milling,[48] and patterning techniques such as electron-beam lithography to produce nanoribbons are a few examples of top-down processes for CNTs and graphene.[49]

Currently, CVD is the predominant technique for CNT synthesis (**Fig. 4**), owing to its ability to provide accurate structural control of CNTs and to enable large-scale production.[50] On a small scale, the process is carried out in a quartz reactor, into which a carbon-containing gas or liquid, such as acetylene,[51] ethylene,[52] liquid hydrocarbons (*e.g.*, toluene,[53] xylenes[54]), or alcohols[55] is introduced as the carbon source. CVD is typically a catalytic process in which Ni-, Co-, and/or Fe-based catalysts are commonly used.[56]

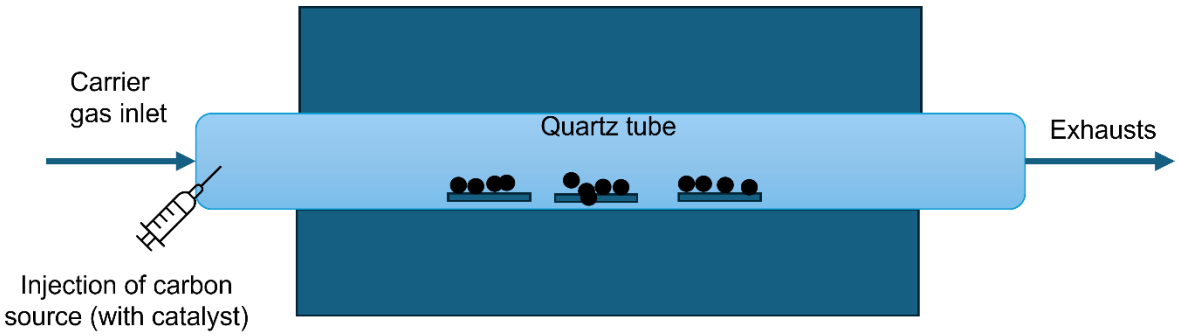

Fig. 4 Scheme of CVD.

In this process, high temperatures (600-1200 °C) are used to decompose the carbon feedstock and to synthesise CNTs on the surfaces of metallic catalyst particles.[57] By controlling the temperature, one may influence the diameter and growth rate of CNTs.[58] For the large-scale production, fluidised bed chemical vapour deposition (FBCVD) reactors are employed. The upward gas flow in a vertical reactor fluidises the catalyst particles.[59] This processing enhances contact between particles, improving both process efficiency and cost-effectiveness. The reactor architecture also enables scalability, making it ideal for producing CNTs in large quantities.[60] Numerous variations of the CVD method exist, including plasma-enhanced CVD,[61] hot filament CVD,[62] radio frequency[63] and microwave-enhanced CVD.[64] Additionally, water-[65], carbon dioxide-[66], oxygen-[67], and ethanol-assisted[68] CVD have been studied. The comparison of the frequently used methods for CNTs synthesis is presented in **Table 1**.

Table 1: Summary of characteristics of the most frequently used methods for CNTs synthesis[69,70]

Characteristics	CVD	Laser ablation	Arc discharge
Condition	High temperature (600-1000 °C)	Argon/Nitrogen gas at 6.6×10^4 Pa	Helium at 6.6×10^3 Pa
Carbon source	Mainly hydrocarbons (liquid or gas)	Pure graphite	Pure graphite
Yield per carbon	<90-95%	80-85%	<75%
CNTs type	Both SWCNTs and MWCNTs;	Only SWCNTs	Both SWCNTs and MWCNTs
Advantages	Low cost, easy scale-up; long CNTs; high purity	High yields, high purity of SWCNTs	CNTs with few defects; No catalyst needed
Disadvantages	Carbon sources may be hazardous	High cost	High cost, short and entangled CNTs are obtained; very often, the produced CNTs must be purified.

CVD is also one of the most widely used techniques for producing high-quality graphene, particularly for applications that require large area, uniform films. Thin films or foils of metals like copper or nickel are the most widely used substrates for graphene CVD.[71] This is because the surface characteristics of these metals have a significant impact on the structure and quantity of graphene layers that are produced. Once the substrate is ready, it is placed inside the CVD reactor and heated to the target growth temperature, typically between 900 and 1050 °C for copper substrates.[72]

Table 2: Summary of characteristics of the most frequently used methods for graphene synthesis[73,74]

Characteristics	CVD	Liquid-phase exfoliation	Mechanical exfoliation	Epitaxial growth
Process condition	High temperatures (900-1050 °C)	Disperse graphite in solvents or surfactant solutions	Physically peel layers from graphite using adhesive tape	Heating of single-crystal SiC (>1300 °C) in vacuum or inert gas
Carbon source	hydrocarbons	graphite	graphite	Ultrathin SiC film
Yield of monolayer graphene	~90%	3-5%	70-95%	1-20 monolayer flakes per cm^2
Graphene type	Large-area monolayer or few-layer graphene films	Graphene flakes (single- to few-layer) in dispersion	Monolayer and few-layer graphene flakes	High-quality, wafer-scale graphene
Advantages	High-quality, continuous sheets, scalability,	Scalable, low-cost, easy processing	Inexpensive and fast, high crystallinity	Excellent crystallinity, uniform films, no transfer needed; suitable for electronic-grade graphene
Disadvantages	Transfer from metal to the target substrate can introduce defects	High range of thickness and flake size; solvent removal needed	Not scalable, random flake size	Expensive substrates, high cost

Additionally, recent studies aim to eliminate petroleum-based feedstocks used in the synthesis of CNTs and replace them with sustainable raw materials such as essential oils,[75] plant extracts,[76] or agricultural biomass.[77] This change is part of a broader strategy of reducing dependency on fossil fuels while valuing inexpensive, abundant, and frequently waste-derived natural resources. However, there are still obstacles to overcome to scale up these green synthesis pathways to industrial levels, such as controlling structural parameters and achieving consistent CNT quality.[78] Simultaneously, new synthetic approaches are being developed. For instance, desired CNT products were directly produced from collected carbon dioxide *via* molten-salt-based CO_2 electrolysis.[79] This method demonstrates how the manufacturing of nanomaterials, carbon capture and utilisation can be combined to transform greenhouse gases into valuable carbon nanostructures.

1.2. Properties and applications of CNTs and graphene

Because of their unique structures, **individual graphene and CNTs** have exceptional mechanical, optical, magnetic, thermal, and electrical properties. Some applications of CNTs and graphene are shown in **Fig. 5**. sp^2-Nanocarbons have a remarkable strength-to-weight ratio due to their low atomic mass and strong bonds. For this reason, individual CNTs and graphene perform better than steel, Kevlar®, and even diamond.[80] The tensile strength of graphene was found to be 130 GPa (mechanically exfoliated graphene membrane measured by the use of nanoindentation in an atomic force microscope (AFM))[32]. For SWCNTs, the tensile strength was found to be 52 GPa, and for MWCNTs, it was 63 GPa (the force was read from the deflection of the calibrated AFM cantilever, whereas the elongation was measured from SEM images).[81] These values are far greater than those of steel (~1-2 GPa).[82] Graphene and MWCNTs exhibit tremendous stiffness, as seen by their Young's modulus of approximately 1 TPa (similar to diamond).[81] The elastic strain limit of graphene is 20–25%,[83] while that of CNTs is roughly 10–16%.[84] Therefore, graphene and CNTs have been used in a variety of

materials engineering domains. In polymer composites,[85] ceramics,[86] and metals,[87] they are used as reinforcing agents to greatly increase their resistance to deformation and fracture.[88] Carbon nanoparticles are also used in lightweight, long-performing, structural components for the automotive,[89] aerospace,[90] and space industries,[91] because of their exceptional strength-to-weight ratio. Furthermore, the addition of carbon nanomaterials to coatings results in markedly improved resistance to scratches,[92] impacts,[93] and abrasion.[94]

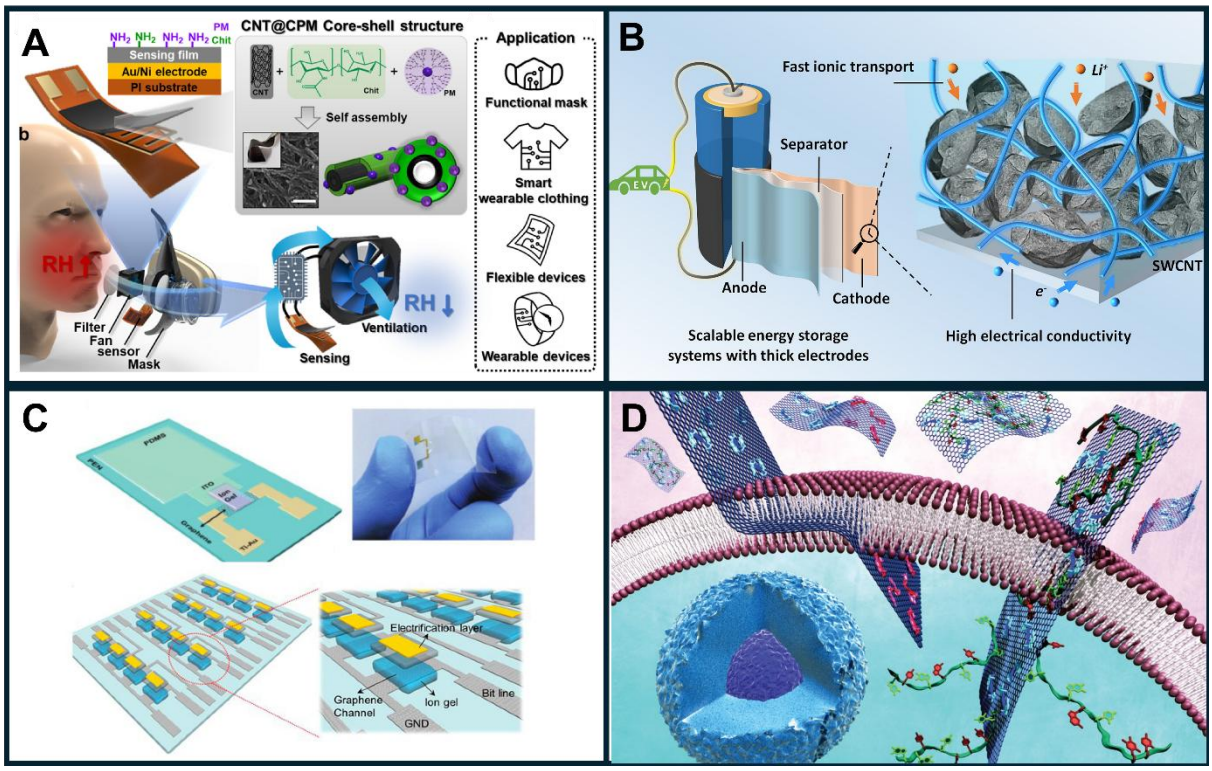

Fig. 5 Application of CNTs or graphene: (A) Flexible and highly sensitive humidity sensors based on wearable CNTs nanocomposite for real-time monitoring of multiple respiratory indicators (Reproduced by permission of Springer (CC-BY 4.0)[95]; (B) Thick SWCNTs-based electrodes for energy storage[96]; (C) Graphene-based tribotronic transistor (Reproduced by permission of Elsevier (Permission number: 6138960512920))[97]; (D) Graphene delivering drugs into the inside of a cell (Reproduced by permission of Springer Nature (Permission number: 6138960274014)).[98]

Applying a current annealing of the suspended graphene and maintaining a measurement environment like a high vacuum (<$5 \cdot 10^{-5}$ mTorr) and low temperature (5 K) allowed to reach charge carrier mobilities of graphene of up to 200 000 $cm^2 \cdot V^{-1} \cdot s^{-1}$.[99] The intrinsic electrical conductivity was found about 10^6 $S \cdot m^{-1}$.[34] Individual metallic SWCNTs can reach conductivities between 10^6-10^7 $S \cdot m^{-1}$ and maintain current densities above $10^9 A \cdot cm^{-2}$. In general, MWCNTs have slightly lower conductivities, typically between 10^5 and 10^6 $S \cdot m^{-1}$.[100] CNTs are used in nanoelectronics as field-effect transistors,[101] whereas graphene is being investigated for applications in flexible circuit designs[102] and high-speed electronic devices[103] because of its extraordinarily high carrier mobility. Both nanomaterials are ideal candidates for chemical[104] and biosensing[105] applications due to their remarkable sensitivity to environmental stimuli. Additionally, mechanical flexibility and transparency of graphene make it a particularly appealing material for solar cells[106] or touch panels.[107] Finally, graphene and CNTs are thought to be potential electrode materials for energy storage devices, such as advanced batteries[108] and supercapacitors.[109]

CNTs and graphene exhibit the highest thermal conductivities ever reported for solid materials, reaching values of several thousand $W \cdot m^{-1} \cdot K^{-1}$. Compared to copper, which has a thermal conductivity of roughly 400 $W \cdot m^{-1} \cdot K^{-1}$, the values for these structures are over an order of magnitude higher.[110] The measured thermal conductivity at room temperature for suspended metallic SWCNTs was found to be 3500 $W \cdot m^{-1} \cdot K^{-1}$,[111] whereas for MWCNTs was 3000 $W \cdot m^{-1} \cdot K^{-1}$.[112] However, the molecular dynamics (MD) simulations revealed even higher values (6600 $W \cdot m^{-1} \cdot K^{-1}$) for SWCNTs.[113] The reduction in the number of walls in MWCNTs enhances heat conduction.[114] For SGL, thermal conductivity is in the range of 3000-5300 $W \cdot m^{-1} \cdot K^{-1}$.[115] Because of these characteristics, graphene and CNTs are becoming more and more significant nanomaterials designable for heat management for contemporary electronics and energy systems. As effective heat spreaders, ultrathin graphene foils or fibres composed of

aligned CNTs stabilise the temperature of integrated circuits,[116] RF/power devices,[117] and LEDs.[118] In polymer composites, elastomers, and 3D-printed materials, the addition of graphene or CNTs increases the thermal conductivity of the overall system.[119,120] When added to phase-change materials (PCMs), graphene or CNTs significantly improve conductivity, reducing heat charge and discharge times and stabilising the structure during melting.[121,122] Additional fields of nanocarbon exploitation include improved flame retardancy,[123] fast thermal sensors and bolometers (low heat capacity, short response time),[124] thin-film heaters for de-icing (CNT/graphene coatings),[125] and battery and power-electronics engineering, where graphene layers minimise the risk of thermal runaway by balancing cell temperatures.[126]

1.3. Dispersion, Network Formation, and Interfacial Compatibility in CNT/Graphene Composites

Despite their excellent properties, the potential of CNTs and graphene remains underexploited. The record-breaking properties of individual nanostructures, such as high electrical and thermal conductivity, excellent mechanical strength, and low weight, rarely translate directly into target components. At the macro level, issues such as contact resistance, aggregation, and poor adhesion at contact surfaces, along with variations in batch quality and process constraints, dominate. The following factors are crucial for achieving truly **(multi)functional composites**: (1) the intrinsic properties of CNTs/graphene, such as thickness (number of layers or walls), lateral size/diameter, interfacial compatibility with the polymer matrix, and sheet and wall quality; (2) the quality of dispersion and spatial distribution within the composite; and (3) the filler loading (**Fig. 6**).

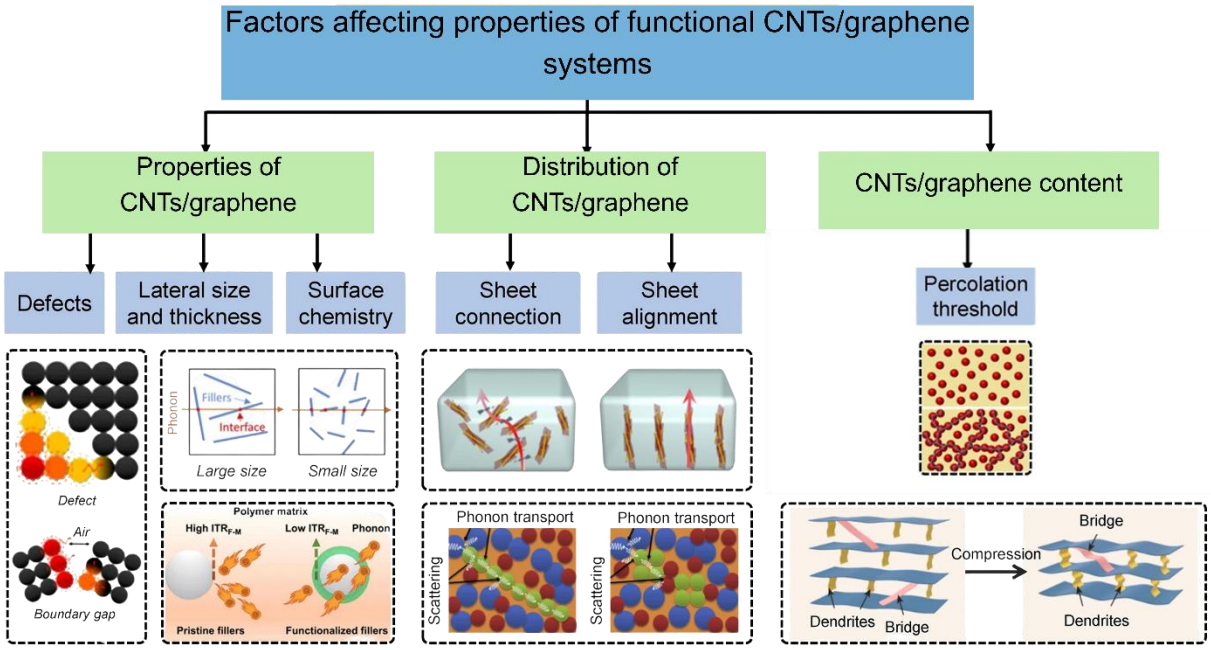

Fig. 6 Determinants of thermal and electrical conductivity in polymer composites with graphene or CNT 3D networks. Reproduced with the permission of Springer (CC BY 4.0).[127]

Both graphene and CNTs can approach *quasi*-ballistic transport over submicron scales.[128] Graphene conducts electricity largely in-plane through its delocalized π-electron network, whereas CNTs conduct along the tube axis. Their thermal conduction is largely phonon-dominated, with exceptionally high in-plane (graphene) and axial (CNT) thermal conductivities when lattices are well-ordered.[129] Therefore, strong electron and phonon scattering may be introduced by defects such as vacancies, oxidation sites (both sp^2 or sp^3 sites), or contamination. These defects also increase contact/junction resistance.[130] Consequently, carrier mobility significantly decreases, and in composites, the network becomes limited by imperfect junctions rather than the intrinsic conductivity of the nanocarbons. Moreover, larger graphene flakes and few-layer sheets, as well as longer, high-aspect-ratio CNTs, reduce edge/junction scattering and lower the percolation threshold, boosting both electrical and thermal performance.[131] High aspect ratio (AR) also enables easier alignment *via* self-assembling. Maintaining the length and

quality of the filler while ensuring pristine CNT interfaces (through low-energy dispersion and minimal defects) is essential to achieve the enhancements.

The development of a **three-dimensional (3D) network** of CNTs or graphene within the matrix is an essential challenge. This network, composed of overlapping bundles of CNTs or connected graphene flakes, appears as a continuous pathway extending throughout the sample (**Fig. 7**).

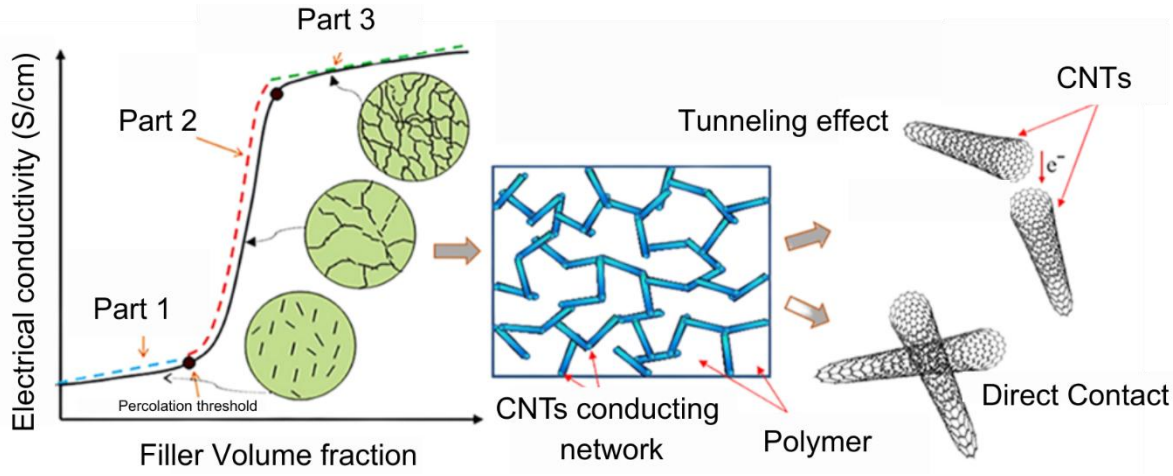

Fig. 7 Dependence of composite electrical conductivity on filler content. Visualisation of conduction *via* physical contacts and tunnelling in a CNT-polymer network. Reproduced with the permission of Elsevier (Permission number: 6138961414253).[132]

Conductive nanostructures start to group and come into contact with one another as the filler loading rises. Most particles connect with their neighbours to form a continuous, sample-spanning 3D-conducting network when a critical concentration, known as the percolation threshold, is reached. At this stage, the composite acts as an electrically or thermally conductive material and offers linked channels for charge transport.[127] Functionally, exceeding the percolation threshold results in a sharp drop in volume resistivity and a step change in thermal and/or electrical conductivity. With an adequate interfacial adhesion, the same network also improves modulus, strength, and damage tolerance. Increased contact density between fillers,

reduced nanometer-scale gaps that promote electron tunnelling and phonon transmission, and strong junctions that efficiently transfer stress from the matrix to the stiff nanocarbon framework lead to a more effective load transfer and enhanced conductivity.[132]

A uniform dispersion of the nanomaterials is necessary to ensure the formation of 3D conductive networks between CNTs or graphene sheets. On the other hand, crosslinking between CNTs or graphene sheets is an additional or complementary method to create a 3D architecture. The formation of chemical or physical links between adjacent nanostructures can be achieved through non-covalent interactions such as π-π stacking,[133] hydrogen bonding,[134] van der Waals forces,[135] or covalent bonding.[136–138]

Homogeneous dispersion in the matrix or liquid ensures uniform formation of conductive paths, effective stress transfer, and maximum utilisation of the contact area between the nanofiller and the surrounding material. This phenomenon enables the production of composites with significantly improved mechanical strength, thermal and electrical conductivity, and structural stability. However, this process is difficult because graphene and CNTs have a strong tendency to form agglomerates due to van der Waals interactions and π-π stacking between carbon planes/sheets.[139,140] Consequently, the particles form dense clusters, limiting effective contact with the matrix and therefore lowering the conductivity. In the literature, there have also been many inconsistencies regarding whether CNTs and graphene are entirely hydrophobic or can become wettable under certain conditions.[141–143] The problem of nonuniform dispersion may be solved by using mechanical methods such as ultrasound or high-shear mixing. However, prolonged ultrasonication may cause defects in the graphene or CNT structures, which reduce their properties.[144] Choosing the right solvent (e.g., *N*-methylpyrrolidone (NMP), *N,N*-dimethylformamide (DMF)) or using a matrix with similar polarity also improves the stability of the dispersion.[145,146] However, another important aspect that must be considered is that, from the technological standpoint, if possible, the solvents with lower toxicity and

volatility are commonly used, especially ethanol or water.[147] Furthermore, reducing the usage of volatile organic compounds or highly toxic substances is consistent with the current movement toward more sustainable and environmentally friendly material processing.

This issue can be resolved by properly altering the surface of nanomaterials. Chemical functionalization, which introduces mainly nitrogen- or oxygen-containing groups to the carbon surface by oxidation or substitution reactions, is one of the most popular methods. Frequently, acid treatments using nitrating mixtures,[148] $KMnO_4$,[149] and piranha solution[150] or amination[151,152] and sulfonation[153] processes are used to introduce carboxyl (-COOH), hydroxyl (-OH), carbonyl (-C=O), amine ($-NH_2$), and sulfonic ($-SO_3H$) groups. This treatment makes graphene or CNTs more hydrophilic and dispersible in aqueous systems. However, the choice between GO and oxidised CNTs does not fully meet the standards of sustainable chemistry, as both require the use of strong oxidising agents. The harsh chemicals pose environmental and health risks, generating hazardous acidic waste and potentially releasing toxic byproducts (NO_x, etc.). Such processes are energy-intensive and conflict with the principles of green chemistry, making them less suitable for sustainable applications. Moreover, the use of strong oxidising agents results in deterioration of the sp^2-nanoarchitecture, thereby hampering the transport of electrons/phonons. As an alternative, non-chemical techniques are employed, such as the adsorption of polymers[154] or surfactants,[155] which stabilise the suspension through steric and electrostatic effects. However, standard surfactants can be toxic to aquatic life, non-biodegradable, and derived from non-renewable petrochemical sources,[156] which makes them not the best candidates for sustainable processing.

To summarise, reducing defect density, eliminating impurities, and suppressing agglomeration or restacking that reduces accessible surface area are critical issues that must be resolved if actual advancements in the use of these nanomaterials are to be made. Developing appropriate interface engineering techniques to guarantee the successful transfer of inherent

qualities into composite systems is equally crucial. Future advancements in controlled synthesis, scalable processing, and targeted functionalization will be essential to unlocking graphene and CNTs full technological potential and paving the way for their integration into next-generation multifunctional materials.

2. AIMS AND SCOPE OF THE WORK

Contemporary research must focus not only on design, fabrication, and integration of graphene and CNTs within polymer and hybrid matrices, but also on scalable, sustainable processing methods. From the perspective of carbon nanostructure processing, which is often a bottleneck for scalable technologies, many problems related to substrate and hydrophilic liquid compatibility arise. There is also a gap in the literature regarding the hydrophobic-hydrophilic properties of carbon-based nanostructures such as graphene and CNTs. Although many studies have focused on the fundamental physicochemical properties of carbon nanostructures, such as morphology, electrical conductivity, thermal conductivity, and mechanical strength, there is still a significant lack of understanding of their behaviour at phase interfaces (*e.g.*, between a carbon nanostructure and a polar or non-polar medium).[157–159]

The goal of the research in PhD dissertation is to take a step towards closing the gap between outstanding properties of individual carbon nanostructures and their utility in composite systems, including Pickering emulsions, phase change materials, or conductive coatings used in textonics. The herein studies explore how effective 3D conductive networks that dictate mechanical, electrical, and thermal properties are formed through controlled synthesis, the presence of defects, dispersion quality, and the interfacial compatibility. A major objective is to establish environmentally responsible routes for producing and processing CNTs and graphene; therefore, mild functionalization or a low-energy regime is presented for the manufacturing of the functional system. The simplicity of the procedure makes it easy to scale up. The work consists of the main part focused on:

- Understanding the amphiphilic properties of graphene [P1] and CNTs [P2] and defining the areas responsible for the amphiphilicity of these materials, which will allow for the maintenance of stable Pickering emulsions.

- Examination of how different CNT morphologies, including AR ratio, number of walls, and degree of crystallinity, affect the thermophysical characteristics of resulting paraffin-based composites as phase change materials [P3].
- Development of a biomimetic method for modifying graphene to give it hydrophilic properties and enable its stable dispersion in water and homogeneous conductive coating with enhanced electrical conductivity [P4].

This work offers essential insights into the structure-property-processing linkages that govern the performance of CNT- and graphene-based composites through deep structural characterisation and macroscopic property evaluation, including key functionalities.

3. RESULTS AND DISCUSSION

3.1. Amphipathic Nature of Graphene Flakes

There is no agreement on whether graphene might be partially hydrophilic. In the literature, one may find reports that pristine graphene[160] may stabilise water-in-oil (W/O) emulsions; however, the authors do not define the structural regions of graphene responsible for these stabilising properties. The common belief that graphene is entirely hydrophobic, non-wettable, and challenging to process led to GO being the first choice.[161] However, GO also fail to preserve the outstanding properties of graphene.[162] This publication [P1] questions the common belief that graphene is entirely hydrophobic. It demonstrates that, even in its 'pure' form (lacking chemical modifications), graphene flakes can be located at oil/water interfaces and enhance the stability of emulsions. Moreover, in this work, the fundamental mechanism governing the stability of water/oil emulsions was investigated. It was also determined how the oil-to-water concentration influences this mechanism. Achieving success in this area could lead to novel methods for integrating graphene into liquid environments (such as inks,[163] coatings,[164] and composites[165]) while minimising the need for extensive chemical alterations (which can often compromise valuable properties).

Herein, two types of flakes were selected: (1) G1 flakes having the thicknesses between 0.3 and 1.7 nm, with around 70% being monolayers, and a specific surface area of about 320 ± 20 $m^2 \cdot g^{-1}$ and (2) G3 flakes exhibiting slightly greater thicknesses (1-5 nm) but a smaller surface area of roughly 130 ± 5 $m^2 \cdot g^{-1}$. The use of two types of graphene enabled the investigation of how the thickness and specific surface area of the flakes affect their behaviour at the oil-water interface and their ability to stabilise emulsions. The initial experiments were not surprising. Graphene was practically non-wettable by water, floating on its surface, while it dispersed immediately in the oil phase, in this case *n*-decane (**Fig. 8A**). The situation changed

when graphene was placed into a biphasic system of *n*-decane and water, and the entire vial was shaken manually (**Fig. 8 B).** Manual shaking resulted in the formation of an emulsion. Graphene flakes likely promoted emulsification by forming an outer shell around the pseudo-spherical structures (**Fig. 8 F, G**).

Furthermore, the specific type of emulsion formed in this system was established. The emulsion droplet is composed of an aqueous core encapsulated in the surroundings of *n*-decane. The emulsion droplets remained stable when introduced into *n*-decane, but they disintegrated immediately and completely upon interaction with water. These experiments suggested the formation of the water-in-oil emulsion (W/O) instead of oil-in-water (O/W) as the literature reported for GO.

In the next step of the research, the effect of flake size and concentration on emulsion properties was examined; therefore, three sets of samples were prepared using different concentrations of G3 and G1 graphene flakes, along with commercial graphite flakes. In contrast to graphene, graphite flakes could not stabilise water/oil emulsions because graphite flakes were too thick and large to form droplet shells (**Fig. 8 E**). Interestingly, G3 flakes produced thermodynamically stable emulsions in the water/oil system even at low concentrations (**Fig. 8 C**), despite having a smaller surface area than G1. At higher concentrations, the droplets became more compact and uniform, though gaps in coverage remained visible. Graphene flakes that were not bound were also seen between the droplets, probably serving as connectors to strengthen the three-dimensional network of droplets. The structure of lyophilised graphene flake assemblies was also examined (**Fig. 8H,I**). Scanning electron microscopy (SEM) images showed only incomplete remnants of droplet shells composed of flakes.

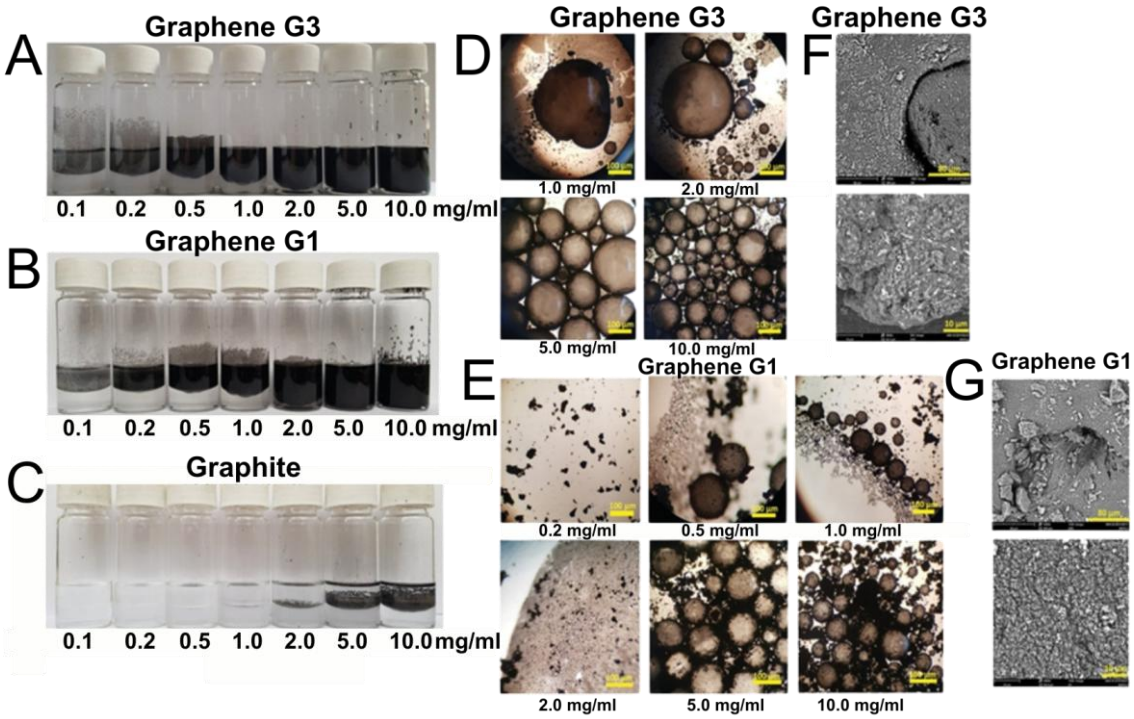

Fig. 8 Formation of water/oil emulsions stabilised by graphene flakes: (A, B) Optical images of Pickering emulsions formed at different concentrations of G3 and G1 graphene flakes in water/*n*-decane mixtures, (C) graphite in a similar water/oil system; (D, E) Optical microscopy images of emulsion droplets stabilised by G3 and G1 graphene flakes. (F, G) SEM images of lyophilised G3 and G1 graphene nanostructures. Reproduced by permission of Wiley. (CC-BY 4.0).[166]

The experiments clearly demonstrated that graphene could stabilise water-oil emulsions and that the type of emulsion obtained differs from those stabilised by GO. As a result, the subsequent phase of the study aimed to investigate the mechanism underlying the amphiphilic properties of graphene flakes. To do that, in line with my experiments, Dr Karolina Milowska (University of Cambridge, CIC NanoGUNE) performed density functional theory (DFT) calculations, MD simulations, and Monte Carlo (MC) simulations. Primary, DFT calculations were employed to evaluate the interaction energy (E_{int}) between graphene flakes, water, and *n*-decane. To this end, eight graphene flakes were analysed. For those systems, DFT revealed more negative E_{int} values for the oil interactions with the basal surface of the flake than with

the edges. Variations in the interaction energies between different edge types and a *n*-decane molecule were minor compared with the pronounced difference between surface and edge sites. Water molecules tend to interact with the edges of the flake rather than its basal surface. These findings clearly demonstrate that the basal plane of graphene flakes is hydrophobic, whereas their edges exhibit hydrophilic character (**Fig. 9 B**).

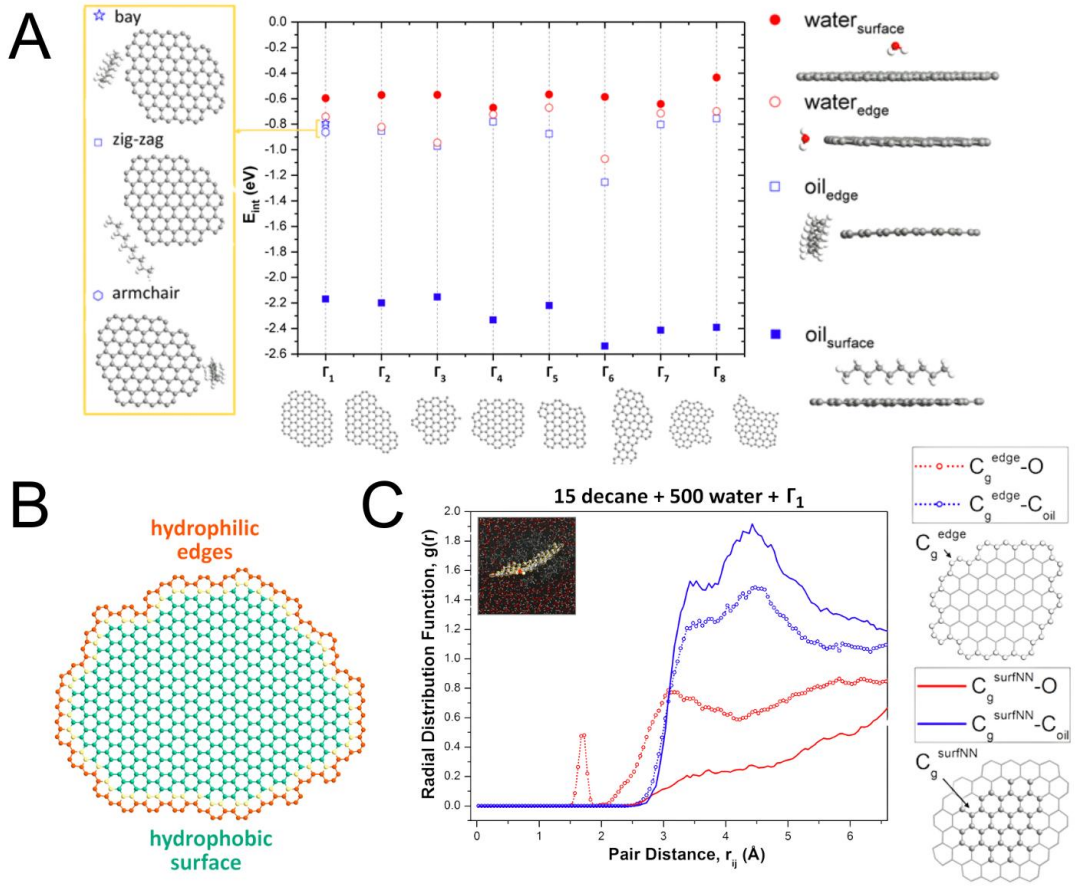

Fig. 9 Interactions between graphene flakes and oil-water systems: (A) DFT-based evaluation of interaction energies in eight small graphene structures; (B) A schematic illustration of graphene amphiphilic nature; (C) Radial distribution functions (RDFs) for edge carbon-water oxygen, surface carbon-water oxygen, edge carbon-oil carbon, and surface carbon-oil carbon pairs. A snapshot of the final simulation state is displayed in the inset. Reproduced by permission of Wiley. (CC-BY 4.0).[166]

Further, MD simulations of all small flakes in oil/water mixtures were carried out. All of these simulations consistently show that water molecules favour interactions with the flake edges, while oil molecules are predominantly positioned above and below the basal plane (**Fig. 9 C**). Notably, the graphene flake is no longer completely flat. This asymmetric adsorption generates uneven stresses across the flake: edges experience stronger polar interactions with water, while the basal plane is 'pushed/pulled' by oil molecules.

Next, it was compared with the experimental results to determine whether the amphiphilic behaviour of graphene flakes depends on their size. We have designed 2 larger flakes, Γ_A and Γ_B, and carried out MD, which proved our hypothesis that flake-solvent interactions are indeed influenced by flake size. As the flake size grows, the probability of finding a water molecule close to its edge becomes lower. Moreover, as flake size increases, the difference in interaction strength between oil molecules and edge carbons versus surface carbons becomes smaller. These results corroborate the hypothesis that smaller flakes have a more pronounced amphiphilic nature.

Further, it was experimentally determined whether the oil-to-water ratio affects emulsion stability. A series of solution experiments in which the graphene mass and the water volume were held constant was conducted. Meanwhile, the volume of *n*-decane was varied from 0 to 4 mL. This variation led to a shift from an unstable regime, characterised by loosely formed emulsions, to a stable regime with densely packed emulsions (**Fig. 10 B**). The critical transition

point was observed at a lower oil concentration for water/G3 mixtures (0.75 mL) than for water/G1 mixtures (1.5 mL) (**Fig. 10 C**).

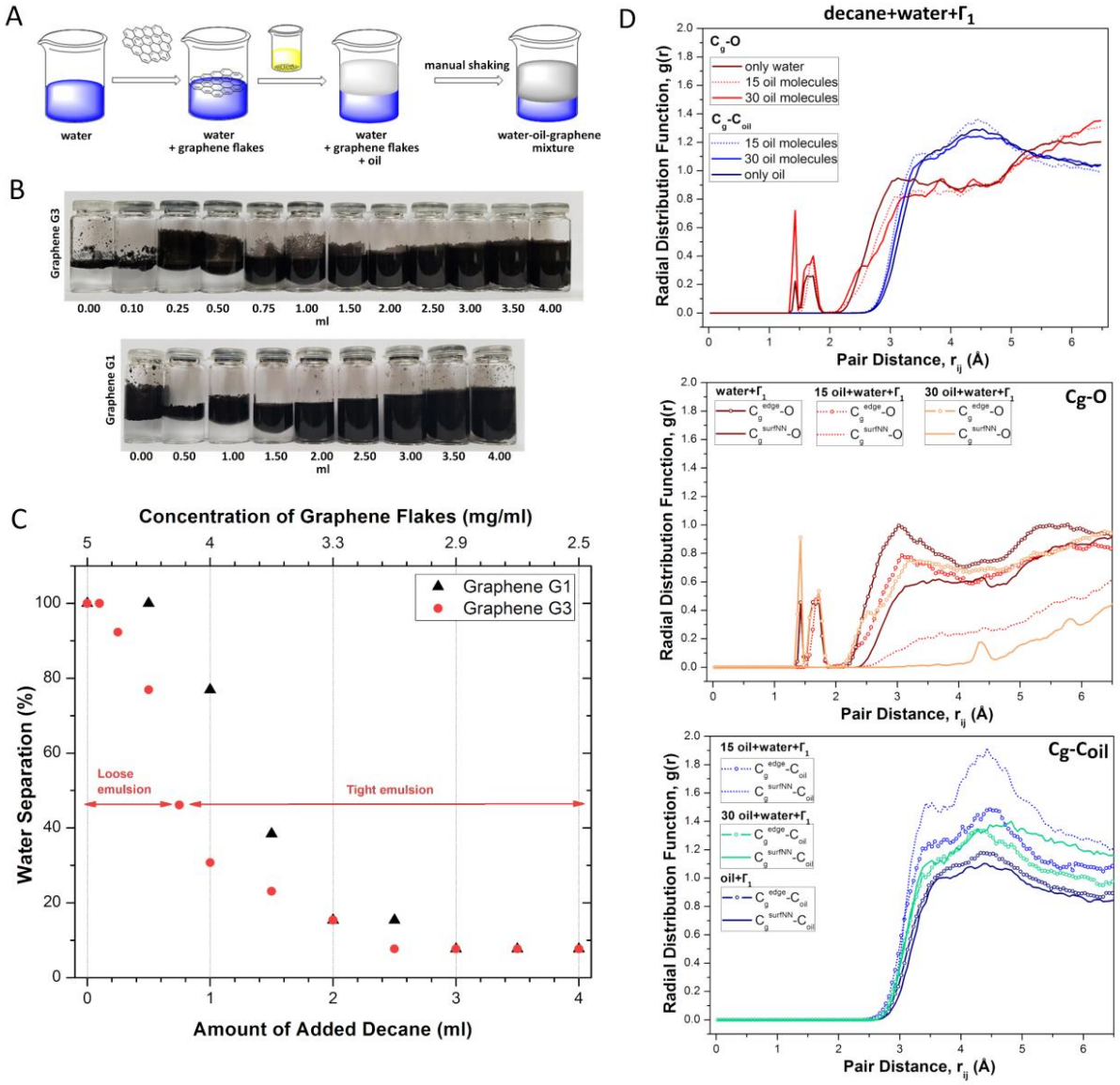

Fig. 10 Influence of the oil-water ratio on the stability of W/O emulsions: (A) Scheme of preparation of the emulsion stabilised by graphene flakes; (B) Optical images of Pickering emulsions with different *n*-decane amounts formed with the used of G3 and G1 graphene flakes; (C) Graph showing the percentage of aqueous phase separation as a function of the amount of added *n*-decane, (D) RDFs of Γ_1 flakes under various oil-water ratios at 300 K and 1 bar. Reproduced by permission of Wiley. (CC-BY 4.0).[166]

Again, working in parallel with Dr Karolina Milowska, the MD determined that the systems with and without oil show that the minimum distance between flake carbons and free water oxygens decreases in the presence of oil but increases progressively as oil concentration increases. This finding indicates that the amphiphilicity of these nanostructures depends more on environmental conditions. In practice, this implies that emulsion stability can be controlled by simply adjusting the oil-to-water ratio.

The stability over time of graphene G3 stabilized water/*n*-decane emulsions was also verified. The emulsion remained stable even after 6 months because G3 flakes create cohesive interfacial films that serve as efficient physical barriers at the oil-water interface by preventing droplet coalescence. This behaviour sets graphene flakes apart from many traditional molecular surfactants, which are susceptible to desorption and instability under comparable conditions. Changing the *n*-decane to toluene (a nonpolar but aromatic solvent) does not affect the ability of graphene flakes to stabilise emulsions. The results clearly showed that changing the solvent did not affect the emulsion stability. Moreover, in the literature, one may find studies that use heptane[167] and even ordinary cooking oil[160] instead. MD simulations also showed that graphene flakes interact similarly with both *n*-decane and toluene. Water molecules are mostly found close to the edges of the flake, whereas oil molecules tend to be found above and below it.

To summarise, in all of these experiments, it was demonstrated that graphene flakes behave as true 2D amphiphiles with distinctly defined hydrophilic and hydrophobic regions. The ratio of edge to surface atoms determines the amphiphilic characteristics of graphene, which are diminished as their size increases due to the diminishing contribution of hydrophilic edges. Therefore, the only flakes that can successfully stabilise water/oil mixtures are those that fall within a specific lateral size range, large enough to maintain stability and small enough to maximise edge effects. It was also shown how altering the oil-to-water ratio can regulate the stability of water/oil emulsions stabilised by graphene flakes.

3.2. Amphipathic Nature of Short and Thin Pristine Carbon Nanotubes

After understanding the mechanism of emulsion stabilisation by graphene, the next natural step was to examine whether other nanocarbon forms also exhibit amphiphilic properties. This time, the experiments began with 1D carbon forms, *i.e.,* CNTs, including both MWCNTs and SWCNTs. Chosen CNTs differed not only in the number of walls but also in their length, diameter, and number of defects. The literature reports some evidence of pristine CNT-stabilised water- oil emulsions.[168] Nevertheless, the majority of research continues to concentrate on the functionalized CNTs.[169–171] The specific structural region of pure CNT that contributes to emulsion stability has not yet been determined. In the publication [P2], it was demonstrated that CNTs possess distinct hydrophilic and hydrophobic regions, thereby exhibiting one-dimensional amphiphilic properties.

The study began with the selection of representative CNTs differing in the number of walls and morphology to verify the influence of the size on the possible amphiphilic properties, *i.e.* SWCNTs Tuball™ (length=5 μm, diameter=2 nm), in-house synthesised MWCNTs (length=770 μm, outer/inner diameters=70/30 nm) and Nanocyl NC7000™ MWCNTs (length=1.5 μm, outer/inner diameter=10/5 nm, 9 wt.% Al_2O_3, 1 wt.% Fe phases). Additionally, (1) purified Nanocyl NC7000™ MWCNTs by the two-step acid-base protocol and (2) oxidised Nanocyl NC7000™ MWCNTs using the nitrating mixture were used. The experimental setup followed assumptions similar to those used for graphene. Upon manual shaking, some of the studied MWCNTs (pristine, purified, and, for comparison, also oxidised Nanocyl NC7000™ MWCNTs) formed stable emulsions. These emulsions were most stable when prepared from purified MWCNTs. An optical microscope was used to show spherical structures of the emulsion droplets. The determined emulsion type for the pristine and purified Nanocyl NC7000™ MWCNTs was O/W; however, for the oxidised MWCNTs, the emulsions were W/O, which shows some similarity to GO. The emulsion made from pristine MWCNTs exhibited

stability for several hours, whereas the emulsion made from purified MWCNTs remained stable for 1.5 months before collapsing, as determined visually. This simple approach indicated that short MWCNTs behave like amphiphilic species.

To link the properties enabling emulsion stabilisation with the CNT surface, the next step in the research was to determine the wettability angle of films made from the studied CNTs. The correlation is shown in the **Fig. 11**.

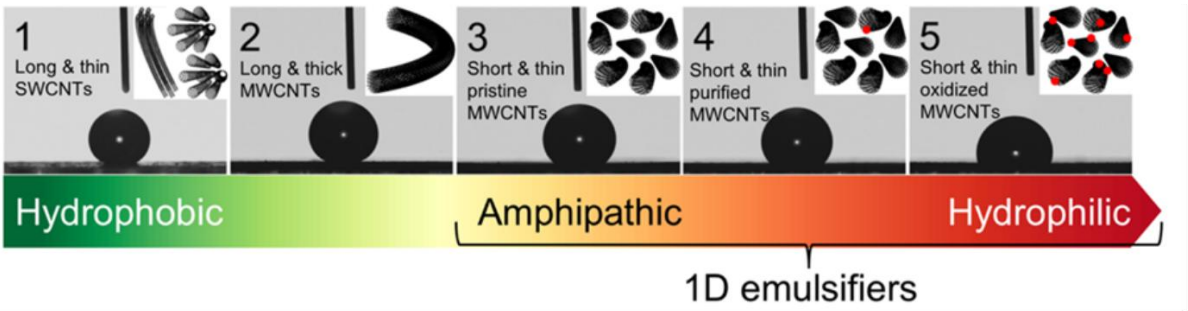

Fig. 11 Wettability investigations of CNT films with different morphological and surface physicochemical properties. Reproduced by permission of Wiley. (CC-BY 4.0).[172]

The analysis of water contact angle (WCA) showed that long and thin Tuball SWCNTs, as well as long and thick in-house MWCNTs, were extremely water-repellent (WCA ~161° and ~157°, respectively), which explains why no emulsion was obtained when these tubes were used. Whereas pristine and purified Nanocyl NC7000™ MWCNTs, which are short and thin, displayed amphipathic behaviour to stabilise O/W emulsions (WCA ~140° and ~133°, respectively). The most hydrophilic CNTs were oxidised Nanocyl NC7000™ MWCNTs (WCA ~108°), leading to a reversal of the emulsion type to O/W.

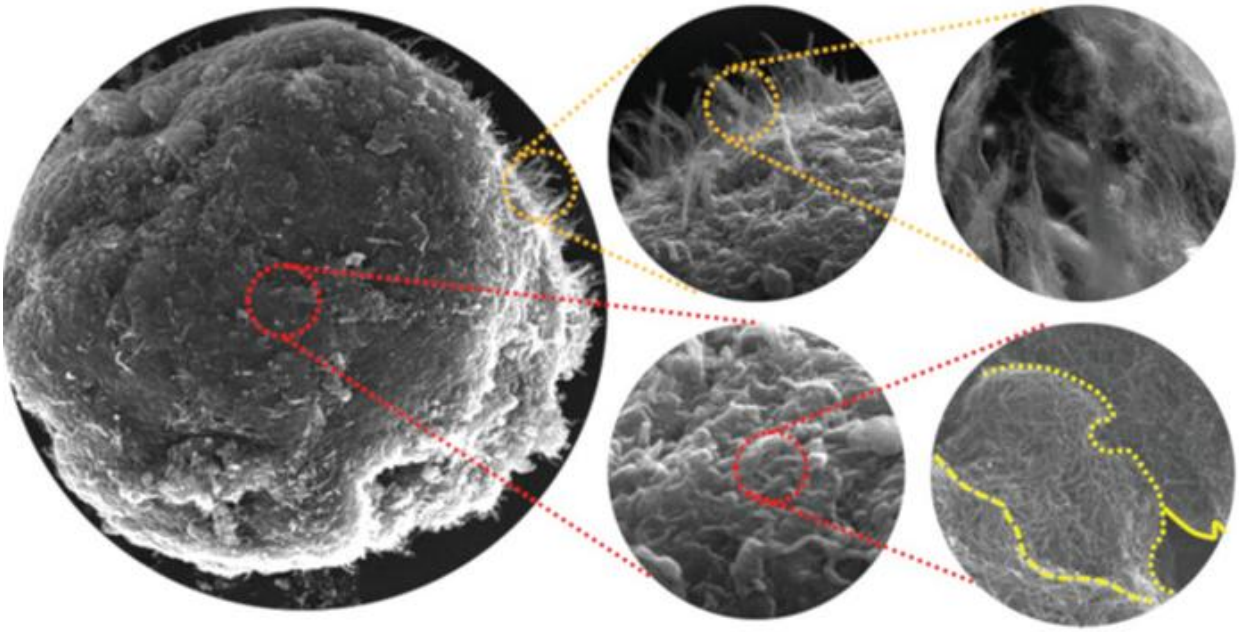

Fig. 12 SEM images of CNT fragments self-assemble into nanostructured shells. Reproduced by permission of Wiley. (CC-BY 4.0).[172]

As the next step, SEM was used to analyse how CNTs spontaneously organize themselves into nanostructured shells (**Fig. 12**). This shell was composed of two different constituents: (1) standing, outward-pointing CNTs perpendicular to the surface of the droplet, resulting in increased surface exposure to the oil phase and (2) a series of layered, tightly packed, intertwined nanotubes arranged isotopically, preventing direct interaction between the water droplet and the oil phase. Together, such an arrangement enabled the formation of a 3D network that provides mechanisms to enhance the emulsion stability.

A physicochemical characterisation of CNTs provided a deeper explanation of the mechanisms underlying their interactions with water and oil. For that, transmission electron microscopy (TEM), Raman spectroscopy, and thermogravimetric analysis (TGA) were used. The morphology and purification effectiveness of the MWCNTs were compared. Pristine Nanocyl NC7000™ MWCNTs display residual aluminium-based catalyst particles together with CNT bundles (**Fig. 13 A**).

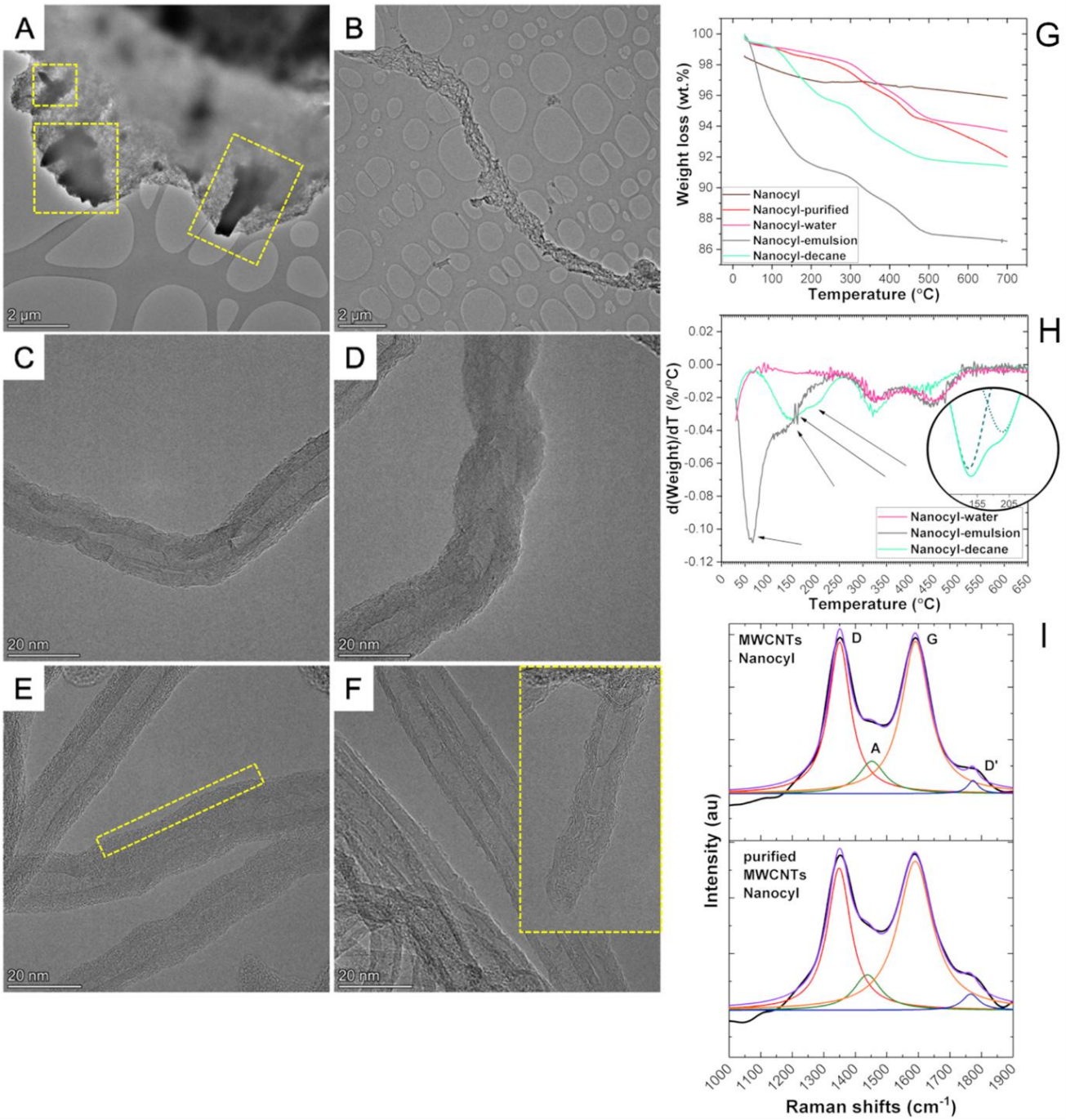

Fig. 13 Analysis of the structural features of pristine and purified MWCNTs: A, C) TEM images of pristine MWCNTs; B, D) TEM images of purified MWCNTs; E) TEM images of MWCNTs extracted from water; F) open-ended MWCNTs isolated from *n*-decane; G) TGA curves of different MWCNT samples; H) the corresponding DTG profiles; I) deconvoluted Raman spectra of pristine and purified MWCNTs. Reproduced by permission of Wiley. (CC-BY 4.0).[172]

Upon purification, MWCNTs became more individualised and free of catalyst residues and catalyst support (**Fig 13 B**), but also some new defects in the wall structures were introduced (**Fig. 13 C**) compared to the pristine one (**Fig. 13 B**). The morphology of MWCNTs extracted from water, *n*-decane, or a water/*n*-decane mixture was analysed. When extracted from water, MWCNTs showed increased coarseness, while for those extracted from *n*-decane it was found that *n*-decane molecules were inside the tubes due to possible capillary action through the open ends of CNTs. TGA analysis also revealed that *n*-decane evaporation occurs in two distinct stages: (1) evaporation of *n*-decane adsorbed on the outer wall (T ~150 °C); and (2) evaporation originating from the nanotube interior (T ~195 °C).

An additional key factor is the level of CNT crystallinity. Based on the deconvoluted Raman spectra, the I_D/I_G ratio was determined. Upon purification of Nanocyl NC7000™ MWCNTs I_D/I_G ratio increased from 0.65 ± 0.04 to 0.73 ± 0.03, which indicates a slightly greater number of defects for the purified MWCNTs. Whereas, the majority of the defects were of the sp^3-carbon type ($I_D/I_{D'}$~12.2). Despite the use of harsh conditions for the purification, a slight amount of the carboxylic and phenolic-type groups was introduced.

Further, to explore the origin of CNTs amphipathic character and their ability to stabilise water/oil mixtures, as with graphene, Dr Milowska carried out DFT, MD, and MC simulations on various oil/water/CNT systems. The interaction between water and *n*-decane molecules with different configurations towards CNTs was determined (**Fig. 14**). For water and CNT edges, the value of E_{int} is more negative than for water and the lateral surface of CNTs, indicating that the water molecule is nearer to the edges of the CNT. Oil molecules tend to associate more strongly with the lateral walls of CNTs. The sidewalls of open-ended CNTs exhibited hydrophobic character, whereas their edges displayed hydrophilic behaviour. When CNTs are capped, the cap does not interact with water; however, the oil interacts even more strongly with the cap than with the lateral surface. These findings imply that CNT caps exhibit greater

hydrophobicity than the nanotube sidewalls, and that fully capped CNTs possess only regions of varying hydrophobicity.

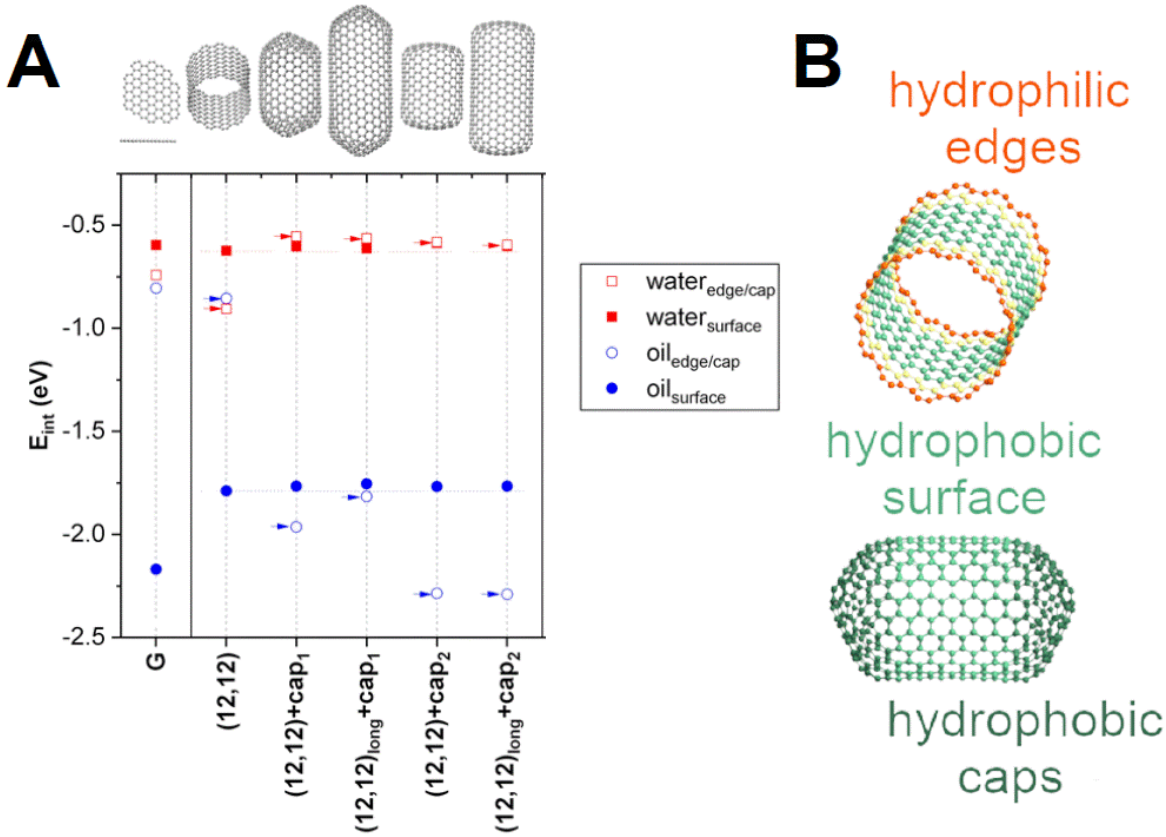

Fig. 14 (A) Interaction energies of open-ended and capped (12,12)-CNTs; (B) Scheme showing the amphiphilic behaviour of open-ended CNTs and the hydrophobic behaviour of capped CNTs. Reproduced by permission of Wiley. (CC-BY 4.0).[172]

Also, the influence of CNT size on their amphiphilic properties was examined. The results were in good agreement with the experiments: shorter, smaller CNTs and those with fewer walls can better stabilise O/W emulsions.

Another important parameter that influences emulsion stability is the oil-to-water ratio. The stability of MWCNTs (2.0 mg·mL^{-1}) in a non-equivolumetric system of water and *n*-decane was examined (**Fig. 15**). Below 20 wt.% and above 56wt.% of *n*-decane the emulsions were not stable. The maximum emulsion fraction was achieved with 32 wt.% of *n*-decane. At higher oil

contents, solvents tend to locate further from the CNTs; therefore, the emulsions become less stable. Also, an increase in the oil-to-water ratio reduces the difference in interaction strength between CNT sidewalls and edges.

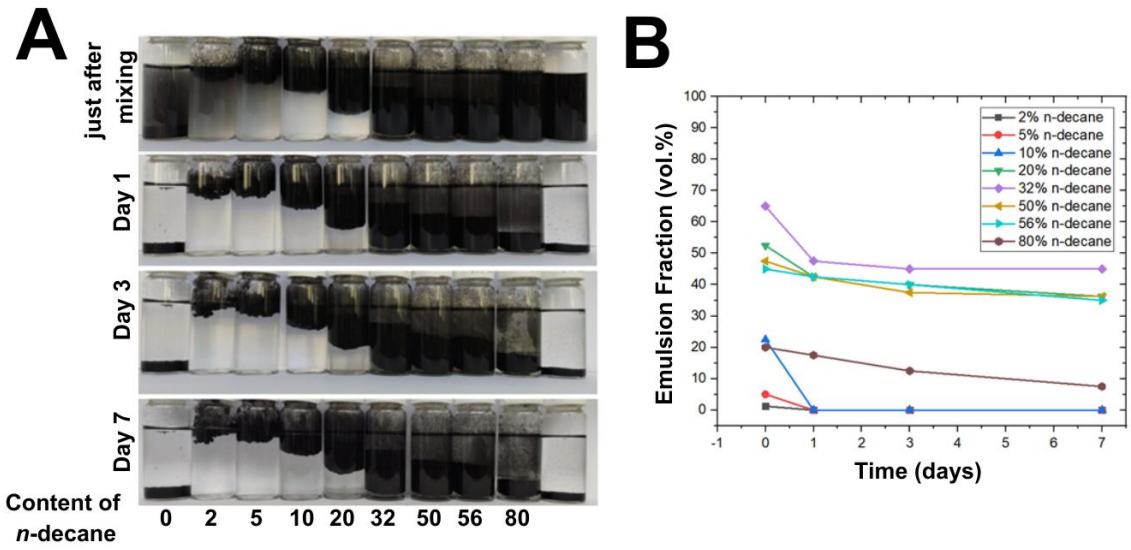

Fig. 15 (A) Emulsions stabilised by purified MWCNTs prepared with *n*-decane/water ratios of 0, 2, 5, 10, 20, 32, 50, 56, 80, and 100 wt.% *n*-decane, imaged directly after mixing and after 1, 3, and 7 days; (B) Time evolution of the emulsion fraction. Reproduced by permission of Wiley. (CC-BY 4.0).[172]

Based on the knowledge about the stability of the emulsions, the paint with the potential application in the flexible textronics were prepared. To ensure a sufficient amount of conductive material for the formation of an optimal conductive network, the concentration of 5 mg·mL^{-1} in *n*-decane:water = 32:68, v/v. The coatings are characterised by a low electrical resistance of 105 Ω (10×5 cm) after 4 layers applied by hand brush (thickness ~ 200 μm).

In summary, the study aimed to unravel the amphipathic nature of thin, short MWCNTs and their ability to stabilise water-in-oil emulsions. Theoretical modelling and experimental techniques verified that CNT edges had a greater affinity for water, while the sidewalls interact preferentially with oil molecules. Hydrophobic domains are linked to the sp^2-hybridised outer

and inner sidewalls as well as the closed caps, while hydrophilic regions are derived from open ends and vacancy defects along with polar functions like carboxyl and phenol-like groups. Their physicochemical characteristics and changes in the oil-to-water ratio can affect emulsion stability. Owing to this anisotropy, short and thin CNTs may, similarly to graphene, act as Pickering stabilisers.

3.3.Carbon nanotube-paraffin composites as heat storage material

The publication [P3] focused on the application of CNTs as a functional filler in paraffin nanocomposites. It was examined how CNTs with different structural features, such as the number of walls and AR, affect the thermophysical behaviour of novel paraffin-based nanocomposites, with a view to their potential use as PCMs. Such improvements are significant since conventional paraffin PCMs suffer from low thermal conductivity and low phase change enthalpy, which limit their large-scale application. Due to their exceptional thermal and structural properties, CNTs offer an efficient means to tailor the heat transfer performance and stability of PCM systems. This approach contributes to the development of advanced energy storage materials suitable for sustainable technologies.

A series of paraffin-based nanocomposites with nanofiller concentrations of 0.5, 1, 2, 5, or 10 wt.% was prepared by melting. Similarly to the previously described study, three types of CNTs were used: Tuball™ SWCNTs, Nanocyl NC7000™ MWCNTs, and in-house MWCNTs. In-house MWCNTs were synthesised using CVD method. To simplify the overall process, carbon nanomaterials were used without catalyst purification. The morphology of all CNTs used in this study was compared, as it is a key factor contributing to the improvement in the thermal conductivity of paraffin-based nanocomposites. As presented in **Fig. 16A-F,** in-house MWCNTs are characterised by a relatively large diameter (60-80 nm) and length (770 μm) compared to Tuball SWCNTs (1.6 nm in diameter and >5 μm in length) and Nanocyl NC7000™ MWCNTs (10 nm in diameter and 1.5 μm in length). The in-house MWCNTs and Tuball SWCNTs tend to align parallel to one another, forming structures that resemble long fibrous strands, whereas the Nanocyl NC7000™ MWCNTs showed a tendency to create coiled, entangled networks that aggregate into bundles.

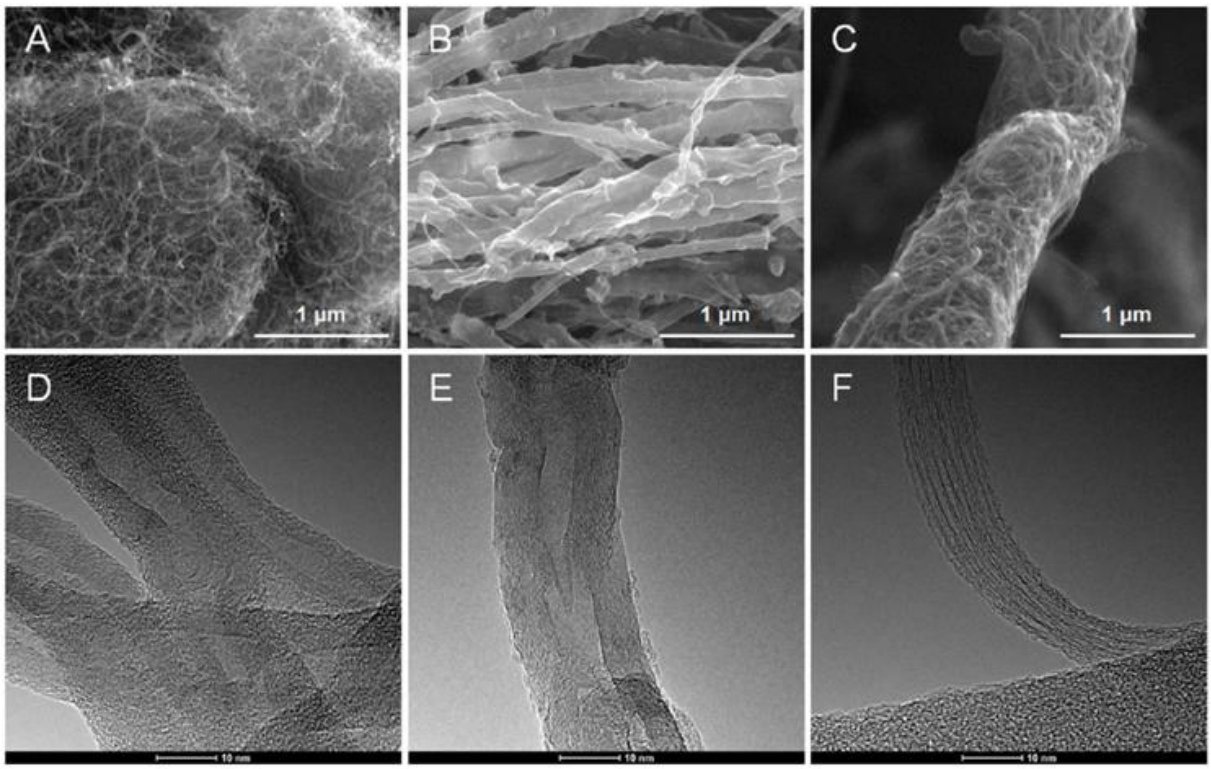

Fig. 16 SEM micrographs of (A) Nanocyl NC7000™ MWCNTs, (B) in-house MWCNTs, and (C) Tuball SWCNTs; and TEM micrographs of (D) Nanocyl NC7000™ MWCNTs, (E) in-house MWCNTs, and (F) Tuball SWCNTs. Reproduced with permission of Elsevier.[173]

Further, the microscopic features of the prepared paraffin-based nanocomposites were analysed. Using the melting procedure, homogeneously dispersed solid nanocomposites were obtained without the use of any additional stabilisers. SEM analysis also revealed different arrangements of CNTs within the nanocomposite, like protruding ribbons for longer CNTs (in-house MWCNTs or Tuball SWCNTs) or tangled web-like structure (Nanocyl NC7000™ MWCNTs) (**Fig. 17A-D**).

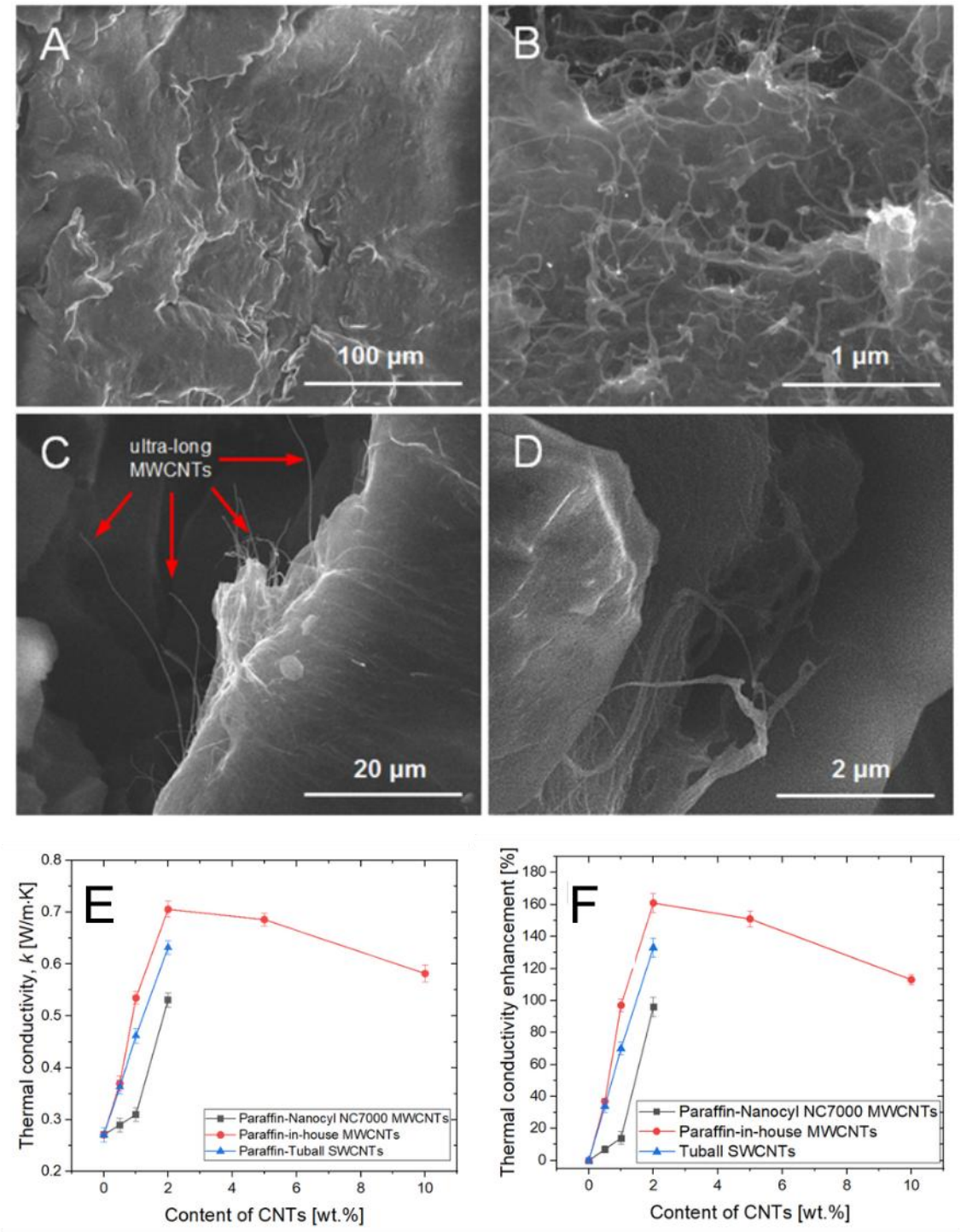

Fig. 17 SEM images of the nanocomposites: (A) pure paraffin; (B) paraffin with 2.0% Nanocyl NC7000™ MWCNTs; (C) paraffin with 2.0% in-house MWCNTs; (D) paraffin with 2.0% Tuball™ SWCNTs; (D) Thermal conductivity of paraffin-based nanocomposites; (E) Percentage improvement in thermal conductivity of paraffin nanocomposites relative to pure paraffin. Reproduced with permission of Elsevier.[173]

In the next step, the thermal conductivity of pristine paraffine and paraffin-CNT nanocomposites was measured. The thermal conductivity of pure paraffin was 0.271 $W \cdot m^{-1} \cdot K^{-1}$. The addition of CNTs contributed to the improvement of the thermal conductivity of paraffin, reaching the maximum value at 2 wt.% of CNTs loading for all types of CNTs (**Fig. 17 E**). In-house MWCNT nanocomposites demonstrated the most favourable performance, reaching over 1.5x improvement of thermal conductivity at 2.0 wt.% loading of CNTs (**Fig. 17 D**). This represents a remarkable achievement compared to the data reported in the literature (**Fig. 18**), as the in-house MWCNTs showed the greatest improvement in thermal conductivity among all MWCNT nanocomposites.

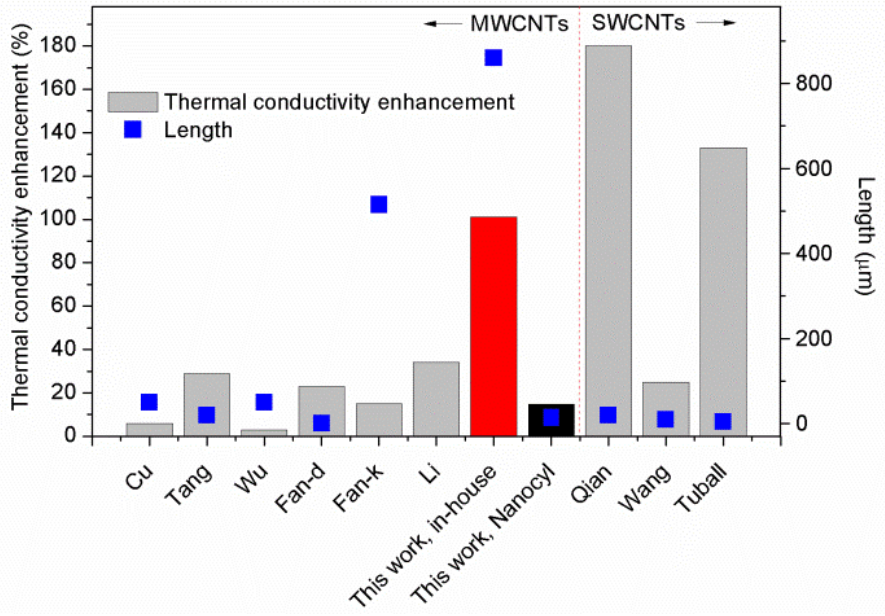

Fig. 18 The thermal conductivity enhancement of our work CNTs was compared against literature data. For MWCNTs, the comparison was made for nanocomposites containing 1 wt.% of CNTs, while for SWCNTs, the reference point was 2 wt.% of CNT loading. Reproduced with permission of Elsevier.[173]

Furthermore, the supercooling temperature of the nanocomposites (**Table 3**) was determined**.** Supercooling temperature of the pure paraffine was 3.9 °C, whereas the addition

of the nanofillers allowed it to be reduced to 2.4 °C (MWCNTs Nanocyl-0.5 wt.%). Here, CNTs could function as nucleating agents, promoting faster crystallisation.

Table 3: DSC test data of PCM nanocomposites. Reproduced with permission of Elsevier.[173]

	onset $T_{heating}$ (°C)	**onset $T_{cooling}$ (°C)**	**peak $T_{heating}$ (°C)**	**peak $T_{cooling}$ (°C)**	**$\Delta H_{heating}$ (kJ/kg)**	**$\Delta H_{cooling}$ (kJ/kg)**
Paraffin	50.24 ± 0.07	54.10 ± 0.15	56.20 ± 0.45	50.57 ± 0.84	150.06 ± 0.23	154.18 ± 0.22
MWCNTs Nanocyl-0.5%	49.89 ± 0.03	52.25 ± 0.09	56.24 ± 0.50	49.84 ± 0.83	152.68 ± 0.39	157.84 ± 0.36
MWCNTs Nanocyl-1.0%	50.16 ± 0.10	54.37 ± 0.16	56.57 ± 0.50	50.45 ± 0.83	151,76 ± 0.69	161.73 ± 0.42
MWCNTs Nanocyl-2.0%	49.87 ± 0.04	54.23 ± 0.09	55.75 ±0.34	49.96 ± 0.85	157.68 ± 0.18	158.83 ± 0.34
MWCNTs in-house-0.5%	49.93 ± 0.01	54,28 ± 0.08	56.31 ± 0.43	50.03 ± 0.85	159.47 ± 0.14	163.54 ± 0.26
MWCNTs in-house-1.0%	47.42 ±0.05	55.82 ± 0.08	52,22 ±0.65	51.05 ± 1.07	150.23 ± 0.61	152.22 ± 0.15
MWCNTs in-house-2.0%	50.13 ± 0.12	54.15 ± 0.11	56.79 ± 0.61	50.45 ± 0.69	146.12 ± 0.36	156.94 ± 0.16
SWCNTs Tuball-0.5%	50.03 ± 0.02	54.48 ± 0.07	55.84 ±0.35	51.15 ± 0.68	158.83 ± 0.15	163.16 ± 0.29
SWCNTs Tuball-1.0%	47.64 ± 0.06	56.31 ± 0.11	56.79 ± 0.57	52.18 ± 0.86	148.35 ± 0.51	149.34 ± 0.58
SWCNTs Tuball-2.0%	50.18 ± 0.026	54.58 ± 0.120	55.65 ± 0.37	51.40 ± 0.67	159.06 ± 0.07	160.69 ± 0.13

The phase change enthalpy also increased by about 6% for in-house MWCNTs and Tuball SWCNTs at 0.5% and 2.0% loading, respectively. Moreover, the 2.0 wt.% in-house MWCNT composite exhibited extreme stability over 50 cycles of subsequent heating and cooling. No aggregation was observed during the test. Both in-house MWCNTs and Tuball SWCNTs enhanced thermal stability by delaying decomposition to higher temperatures (**Fig. 19 B**). These higher enthalpies may result from the increased crystallinity of the CNTs and the paraffin, as well as from the 3D connections of the CNTs, their shape (i.e., aspect ratio), and their overall arrangement. The crystallinity of the studied CNTs was characterised using Raman spectroscopy and X-ray diffraction (XRD). Nanocyl NC7000™ MWCNTs are the most defective structure (I_G/I_D=0.54), in-house MWCNTs (I_G/I_D=1.48) with the moderate

graphitisation degree, but high anisotropy as determined by XRD, whereas the highly ordered structure can be assigned to Tuball SWCNTs (I_G/I_D=13.47).

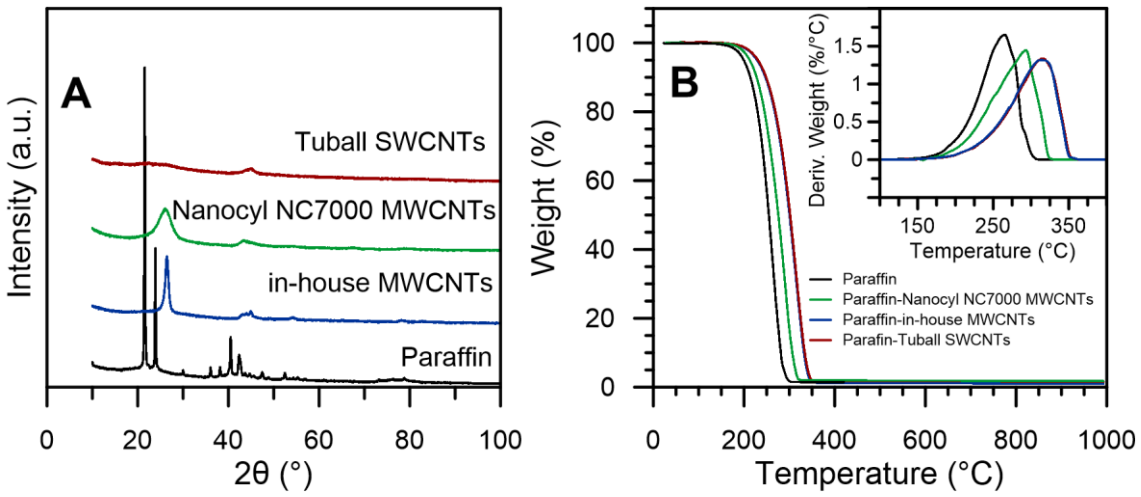

Fig. 19 XRD patterns (A) and TGA curves (B) of the examined CNTs and paraffin-CNT nanocomposites. Reproduced with permission of Elsevier.[173]

To summarise, paraffin-based nanocomposites with various CNTs, differing in dimensions and shape, were prepared. Their overall thermal performance, potentially for use as a PCM energy storage device, was examined. All studied CNTs improved the thermal conductivity of the nanocomposite; however, in-house MWCNTs appear to be the most promising nanofillers (161% enhancement at 2.0 wt.% loading) due to their high AR and enhanced structural order. Both Tuball SWCNTs and in-house MWCNTs increased the phase change enthalpy and simultaneously reduced supercooling. This combination results in a significant overall improvement in the performance of heat storage systems.

3.4. Electroconductive coating based on the L-DOPA modified graphene

In the quest for more sustainable techniques for nanocarbon structure functionalization, recent studies indicate that conventional surfactants can be replaced by naturally derived biomolecules, such as proteins, polysaccharides, and other bio-based macromolecules.[174] Furthermore, biomimetic strategies based on natural adhesion mechanisms have also drawn interest. For example, mussels are known to have exceptional adhesive properties; even under tremendous shear stress from water flow, they may adhere firmly to metal, wood, or stone.[175] Such bio-inspired molecular designs present a promising path toward stable, water-based dispersions and surface modification of graphene or CNTs. In the publication [P4], a new graphene-polylevodopa (PDOPA) hybrid that can be processed in water was synthesised. This approach enabled the production of easily paintable coatings with low surface resistance, which may find use in textronics, radar-absorbing materials (RAMs), or electromagnetic interference (EMI) shielding.

Herein, graphene G3 of the previously depicted characteristics (**Chapter 3.1**) was used.

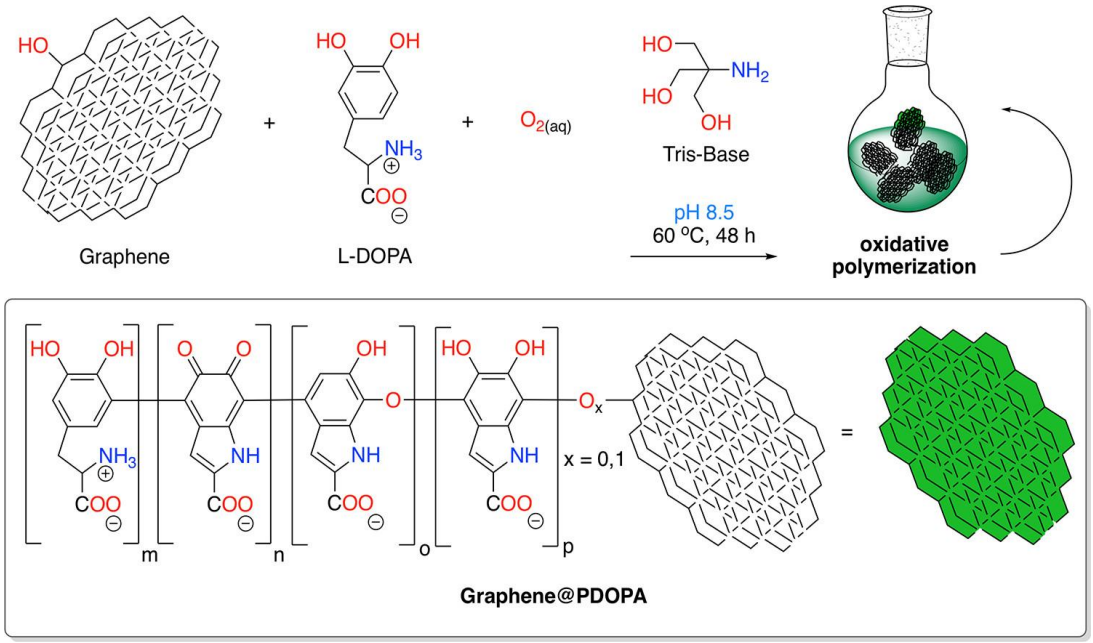

Fig. 20 G3@PDOPA synthesis scheme. Reproduced by permission of ACS (CC-BY 4.0).[176]

Graphene and PDOPA were covalently attached *via* the growth-from polymerisation of L-DOPA (L-3,4-dihydroxyphenylalanine) monomer, as shown in **Fig. 20**. In this oxidative environment, the L-DOPA radicals were coupled with the carbon atom of the graphene flakes (both aromatic and aliphatic) and/or with the hydroxyl oxygens attached to the graphene surface, resulting in negatively charged PDOPA coated graphene. TEM analysis revealed that the G3 graphene was homogeneously coated by the PDOPA (10-20-nm-thick layers).

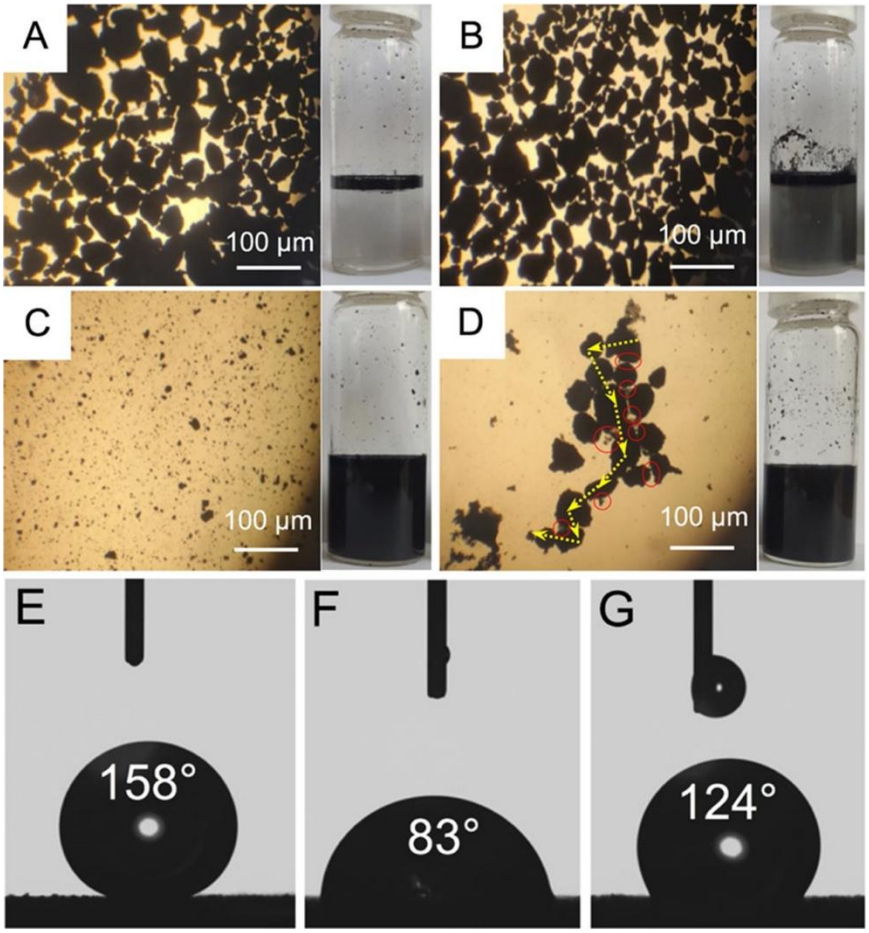

Fig. 21 (A) Micrograph of pristine graphene dispersed in water; (B) micrograph of pristine graphene mixed with L-DOPA in water; (C) micrograph of functionalized graphene (G3@PDOPA) in water; (D) micrograph of a 1:9 (w/w) mixture of G3@PDOPA and pristine graphene; (E–G) WCA measured for graphene G3, PDOPA, and G3@PDOPA, respectively. Reproduced by permission of ACS (CC-BY 4.0).[176]

The dispersion stability of pristine and functionalized G3@PDOPA in water was verified. G3 was non-wettable by water and strongly aggregated (**Fig. 21 A**), whereas the G3@PDOPA yielded homogeneous and over one year stable dispersion in water (**Fig. 21 C**). A control experiment using graphene and non-polymerized L-DOPA was performed. However, such a noncovalent modification did not confer any enhancement (**Fig. 21 B**). Moreover, a mixture of the pristine graphene G3 and G3@PDOPA in the ratio of 9:1 was also prepared, which yielded a stable dispersion because of the formation of 3D network connections between the flakes (**Fig. 21 D**). The dispersion abilities of the studied materials are reflected in the WCA results, which confirm differences in their wettability and interaction with water. The WCA was the highest for the pristine graphene (158°), while after the modification, the G3@PDOPA WCA dropped (123°), which suggests a change in the hydrophilicity of the material. Also, dynamic light scattering (DLS) showed a reduction in the hydrodynamic diameter of G3@PDOPA compared to the pristine G3, which was too large to measure. Moreover, G3@PDOPA dispersion exhibits a highly negative ζ-potential (-25.4 ± 1.52 mV), which is directly related to its stability.

Combustion analysis, FTIR, Boehm titration, TGA, and Raman spectroscopy were also performed to analyse the interaction between PDOPA and the graphene surface. Combustion analysis confirmed that the levels of oxygen (~9%) and nitrogen (~1%) had risen, compared to pristine graphene (97% of C). The oxygen in G3@PDOPA was mainly in the form of carboxylic groups (1.10 $mmol \cdot g^{-1}$) and phenol-like groups (1.75 $mmol \cdot g^{-1}$), and a small amount of lactone groups (0.49 $mmol \cdot g^{-1}$), whereas the content of the amino groups was ~3.20 $mmol \cdot g^{-1}$. The results correlate with the absorption band locations in the FTIR spectra. TGA revealed a high PDOPA content (~23 wt.%) in the functionalized graphene. Moreover, the decomposition temperature of the PDOPA moieties in G3@PODPA shifted to a higher temperature

(300-400 °C) compared to the pristine PDOPA (200-300 °C), indicating the covalent bonding to the graphene surface.

Raman spectra indicated the crystallographic defects introduced by the carbon atoms that participated in addition processes and polymerisation. For G3@PDOPA the I_D/I_G ratio increased to 0.88 (for comparison, pristine graphene exhibited $I_D/I_G \sim 0.54$). Similarly the I_D/I_{2G} ratio, which is a secondary tool for crystallographic defect determination, increased to 0.87 for G3@PDOPA (for pristine graphene $I_D/I_{2G} \sim 0.80$). These results suggest a partial conversion of sp^2-into sp^3-carbon atoms upon functionalization. Also, we have observed shifts in the D- and G-band positions. The G-band for G3@PDOPA was shifted toward higher frequencies (~5 cm^{-1}), indicating that radical trapping during the polymerisation initiation step caused the electrons to retreat from the graphene π-system.

The next stage of the research aimed to demonstrate the application potential of the obtained hybrid materials. For this purpose, paint containing a total graphene concentration of 10% with varying ratios of G3@PDOPA to pristine G3 was prepared. The produced graphene-based paints exhibited desirable shear-thinning behaviour, a feature of high-performance coating formulations. As the shear rate increased, their viscosity decreased dramatically, making them easy to mix and apply. However, they retained sufficiently high viscosity under static conditions to avoid sagging or phase separation. Furthermore, low yield stress indicated sufficient structural stability both during storage and after use.

SEM imaging of the coatings obtained from the prepared paints applied onto a cotton textile was performed. Inhomogeneous coatings with noticeable agglomerates and large voids were produced by a pristine graphene formulation. The coatings containing G3@PDOPA exhibited uniform surface coverage, reduced porosity, and fine distribution of graphene flakes across the fabric, making it suitable for functional textile applications.

To demonstrate the coatings functionality, the sheet resistance of samples with different G3 to G3@PDOPA ratios was measured. For all of the samples, resistance decreased systematically with the addition of successive layers of paints (**Fig. 22**). However, for a coating composed of 10 wt.% of pristine graphene (9.8 kΩ), we obtained a lower resistance value compared to the 10 wt.% G3@PDOPA coatings (27.6 kΩ). The G3@PDOPA exhibited higher resistance due to its high PDOPA content.

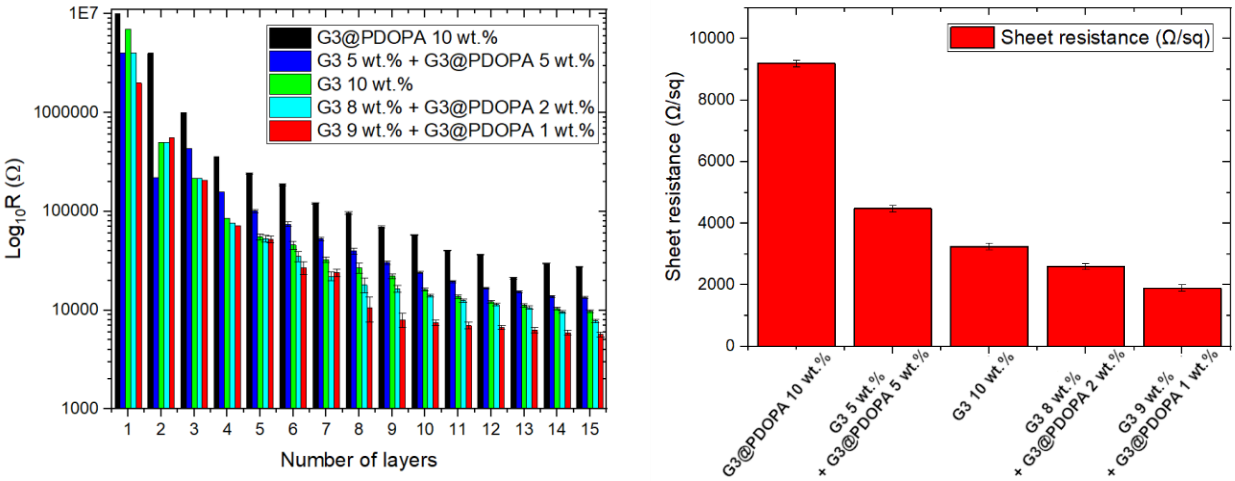

Fig. 22 Electrical resistivity of cotton fabrics coated with graphene-based paints containing a total graphene concentration of 10 wt.% *(left),* and sheet resistance measured after deposition of the final layer *(right).* Reproduced by permission of ACS (CC-BY 4.0).[176]

However, more promising results may be obtained with the combination of G3 and G3@PDOPA in various ratios, where the most promising was 9 wt.% G3 and 1 wt.% G3@PDOPA. Here, the sheet resistance was reduced to 5.7 kΩ, which, after recalculating into sheet resistance, was 1.9 kΩ sq^{-1} or 0.21 Ω·m. In such a case, G3@PDOPA acts as a supramolecular dispersing agent,[177] driven by π-π stacking interactions between graphene and the surfactant-like G3@PDOPA species. As a result, a stable 3D network emerged, leading to strong electrical conductivity and efficient charge-transport paths.

To summarise, it was demonstrated that pristine graphene flakes can be efficiently dispersed by the graphene@PDOPA nanohybrid, allowing the manufacture of stable, long-lasting water acrylic paints. Based on that, flexible, printable or paintable coatings with electrical resistance as low as 1.9 kΩ sq^{-1}, may be created. Such coatings may be applicable in textronics, RAMs or EMI shielding. This mild functionalization enables the elimination of standard surfactants, making the graphene production process more sustainable.

SUMMARY AND FURTHER PERSPECTIVE

The dissertation focused on the application of carbon nanostructures, mainly graphene and CNTs, into functional composites with an emphasis on the sustainable approach. The introduction section describes the processes, structures, properties, and possible applications of the aforementioned 1D and 2D nanomaterials. The main technological challenges associated with processing graphene and CNTs must be addressed to effectively transfer their unique properties from the nanoscale to the macroscale, thereby fully exploiting their potential.

The study of the amphiphilic properties of graphene and CNTs revealed that the structural anisotropy resulting from differences in surface and edge structure plays a key role in their amphiphilic behaviour [P1], [P2]. In both materials, amphiphilic properties are determined by the ratio of hydrophilic areas (associated with edges or defects) to hydrophobic regions (the basal plane). The appropriate selection of graphene flake or CNT size and morphology, along with control of the oil-water phase ratio, allows regulation of the stability of the Pickering emulsions. These results confirm that both graphene and CNTs can act as effective, low-dimensional interfacial stabilisers, eliminating the usage of standard fossil-fuel-based surfactants. Removing many of the drawbacks of existing stabilisers enables these materials to find applications in a wide range of geological, biological, and environmental technologies. Graphene/CNT membranes, aerogels and sponges with switchable wettability (superhydrophobic/superoleophilic) may be used for oil spill removal, wastewater treatment and demulsification.[178] Knowledge of CNTs or graphene amphiphilic properties also enables the design of the drug delivery system (Pickering emulsions as ‘microcapsules’ that protect active substances).[179] Also, such graphene-stabilised Pickering emulsions may be used as microcapsule-based self-healing coatings, which have attracted considerable interest from researchers.[180]

The study of the thermal properties of the CNTs-paraffin nanocomposites containing various types of CNTs revealed that all tested nanostructures increased the thermal conductivity of paraffin even at low concentration [P3]. Among the analysed materials, the most promising were in-house MWCNTs, which, thanks to their high AR and crystallinity, provided a 161% increase in thermal conductivity at a 2.0% by weight content. In addition, both Tuball SWCNTs and in-house MWCNTs increased the phase transition enthalpy and reduced supercooling, thereby improving the stability and efficiency of heat accumulation and release processes. In particular, length, diameter, aspect ratio, and crystallinity of CNTs are crucial for achieving optimal thermal parameters. The results of these studies confirm that properly designed CNT/paraffin composites can significantly improve the efficiency and durability of modern thermal energy storage systems. An interesting area of research in the field of innovative materials is the development and characterisation of microencapsulated phase change materials (MEPCM). Microencapsulation of PCM is a more advantageous solution than its use in an unencapsulated form, as it provides better thermal and mechanical stability and eliminates active material leakage during phase change. Encapsulating the PCM core enables controlled operation and separation from the external environment, significantly extending the system's life and enabling its practical application in coatings, composites, and building materials. For such an encapsulation, graphene or CNT-stabilised Pickering emulsions may be used.[181]

Graphene can be effectively dispersed using a graphene-PDOPA nanohybrid, enabling the production of stable, durable water-based acrylic paints containing graphene flakes [P4]. This enables the production of flexible, conductive coatings that can be printed or applied as paint, achieving a surface resistance of 1.9 kΩ/sq. Mild reaction conditions characterise the proposed graphene modification and avoid the use of conventional surfactants, which significantly improves the sustainability and environmental friendliness of the production process. These results confirm that PDOPA-based nanohybrids are a promising route to the production of

environmentally friendly, functional graphene coatings with broad application potential. Such graphene-based coatings not only enhance electrical conductivity but also create a diffusion barrier that slows down the penetration of oxygen, chloride ions, and water to the metal surface, thus providing effective anticorrosive protection.[182] The strong infrared absorption of graphene enables these coatings to be used in de-icing, heating, or thermal energy storage systems.[183] Moreover, incorporating graphene into resins or varnishes enhances the hardness, wear resistance, and adhesion of coatings.[184] Due to its large specific surface area, graphene can also enhance stress transfer within the composite, thereby improving the mechanical performance and durability of the coating system.

In my PhD dissertation, it was demonstrated that thanks to the amphiphilic nature and anisotropic structure of graphene and CNTs, they can effectively organise themselves at liquid-liquid interfaces, forming stable emulsion systems and spatial 3D networks. These properties can be used to design functional composite materials, in which a 3D network made of graphene or CNTs provides effective electrical and thermal conductivity as well as high mechanical stability. Appropriate adjustment of morphology, size, and surface functionalization allows the unique properties of nanomaterials to be transferred from the nano to the macro scale, enabling their full potential to be exploited in multi-functional applications. In the next stage of research, it would be worthwhile to focus not only on the behaviour and interactions of individual CNTs or graphene flakes within the system, but also on the formation of a continuous 3D network through crosslinking or controlled assembly. Moreover, an interconnected 3D network could further improve charge and heat transport efficiency, leading to higher, more isotropic electrical and thermal conductivities. It may also increase resistance to deformation, cracking, and fatigue, thereby extending the durability of the material under mechanical or thermal stress. Importantly, the degree and nature of crosslinking could be tailored to balance flexibility and rigidity, enabling the design of materials with tuneable mechanical and functional properties.

Overall, exploring strategies for 3D crosslinking of graphene and CNT networks represents a promising direction for developing next-generation multifunctional composites that combine high performance, structural integrity, and environmental stability.

LITERATURE

(1) Sorooshian, S. The Sustainable Development Goals of the United Nations: A Comparative Midterm Research Review. *Journal of Cleaner Production* **2024**, *453*, 142272. https://doi.org/10.1016/j.jclepro.2024.142272.

(2) Popescu, C.; Dissanayake, H.; Mansi, E.; Stancu, A. Eco Breakthroughs: Sustainable Materials Transforming the Future of Our Planet. *Sustainability* **2024**, *16* (23), 10790. https://doi.org/10.3390/su162310790.

(3) Baig, N.; Kammakakam, I.; Falath, W. Nanomaterials: A Review of Synthesis Methods, Properties, Recent Progress, and Challenges. *Mater. Adv.* **2021**, *2* (6), 1821–1871. https://doi.org/10.1039/D0MA00807A.

(4) Mekuye, B.; Abera, B. Nanomaterials: An Overview of Synthesis, Classification, Characterization, and Applications. *Nano Select* **2023**, *4* (8), 486–501. https://doi.org/10.1002/nano.202300038.

(5) Saito, R.; Dresselhaus, G.; Dresselhaus, M. S. *Physical Properties of Carbon Nanotubes*; PUBLISHED BY IMPERIAL COLLEGE PRESS AND DISTRIBUTED BY WORLD SCIENTIFIC PUBLISHING CO., 1998. https://doi.org/10.1142/p080.

(6) Iijima, S. Helical Microtubules of Graphitic Carbon. *Nature* **1991**, *354* (6348), 56–58. https://doi.org/10.1038/354056a0.

(7) *Carbon Nanotubes*; Dresselhaus, M. S., Dresselhaus, G., Avouris, P., Eds.; Topics in Applied Physics; Springer Berlin Heidelberg: Berlin, Heidelberg, 2001; Vol. 80. https://doi.org/10.1007/3-540-39947-X.

(8) Popov, V. Carbon Nanotubes: Properties and Application. *Materials Science and Engineering: R: Reports* **2004**, *43* (3), 61–102. https://doi.org/10.1016/j.mser.2003.10.001.

(9) Charlier, J.-C. Defects in Carbon Nanotubes. *Acc. Chem. Res.* **2002**, *35* (12), 1063–1069. https://doi.org/10.1021/ar010166k.

(10) Liu, Z.-B.; Zhou, Z.-J.; Li, Z.-R.; Li, Q.-Z.; Jia, F.-Y.; Cheng, J.-B.; Sun, C.-C. What Is the Role of Defects in Single-Walled Carbon Nanotubes for Nonlinear Optical Property? *J. Mater. Chem.* **2011**, *21* (24), 8905. https://doi.org/10.1039/c1jm10852b.

(11) Sammalkorpi, M.; Krasheninnikov, A.; Kuronen, A.; Nordlund, K.; Kaski, K. Mechanical Properties of Carbon Nanotubes with Vacancies and Related Defects. *Phys. Rev. B* **2004**, *70* (24), 245416. https://doi.org/10.1103/PhysRevB.70.245416.

(12) Bie, Z.; Deng, Y.; Liu, X.; Zhu, J.; Tao, J.; Shi, X.; He, X. The Controllable Mechanical Properties of Coiled Carbon Nanotubes with Stone–Wales and Vacancy Defects. *Nanomaterials* **2023**, *13* (19), 2656. https://doi.org/10.3390/nano13192656.

(13) Charlier, J.-C.; Blase, X.; Roche, S. Electronic and Transport Properties of Nanotubes. *Rev. Mod. Phys.* **2007**, *79* (2), 677–732. https://doi.org/10.1103/RevModPhys.79.677.

(14) Valdés-Madrigal, M. A.; Montejo-Alvaro, F.; Cernas-Ruiz, A. S.; Rojas-Chávez, H.; Román-Doval, R.; Cruz-Martinez, H.; Medina, D. I. Role of Defect Engineering and Surface Functionalization in the Design of Carbon Nanotube-Based Nitrogen Oxide Sensors. *IJMS* **2021**, *22* (23), 12968. https://doi.org/10.3390/ijms222312968.

(15) Daneshvar, F.; Chen, H.; Noh, K.; Sue, H.-J. Critical Challenges and Advances in the Carbon Nanotube–Metal Interface for next-Generation Electronics. *Nanoscale Adv.* **2021**, *3* (4), 942–962. https://doi.org/10.1039/D0NA00822B.

(16) San, M. T.; Prachakittikul, P.; Chainarong, K.; Sripisarn, T.; Kerdnawee, K.; Suttiponparnit, K.; Charinpanitkul, T.; Koo-Amornpattana, W.; Srifa, A.; Ratchahat, S.; Chaiwat, W. Potential Production of Carbon Nanotubes from Liquid Aromatic Hydrocarbons over Fe and Ni on Alumina Powder via Catalytic Chemical Vapor Deposition. *Diamond and Related Materials* **2023**, *137*, 110130. https://doi.org/10.1016/j.diamond.2023.110130.

(17) Wu, Q.; Qiu, L.; Zhang, L.; Liu, H.; Ma, R.; Xie, P.; Liu, R.; Hou, P.; Ding, F.; Liu, C.; He, M. Temperature-Dependent Selective Nucleation of Single-Walled Carbon Nanotubes from Stabilized Catalyst Nanoparticles. *Chemical Engineering Journal* **2022**, *431*, 133487. https://doi.org/10.1016/j.cej.2021.133487.

(18) Bedewy, M.; Meshot, E. R.; Reinker, M. J.; Hart, A. J. Population Growth Dynamics of Carbon Nanotubes. *ACS Nano* **2011**, *5* (11), 8974–8989. https://doi.org/10.1021/nn203144f.

(19) Kharlamova, M. V.; Paukov, M.; Burdanova, M. G. Nanotube Functionalization: Investigation, Methods and Demonstrated Applications. *Materials* **2022**, *15* (15), 5386. https://doi.org/10.3390/ma15155386.

(20) Lavagna, L.; Bartoli, M.; Suarez-Riera, D.; Cagliero, D.; Musso, S.; Pavese, M. Oxidation of Carbon Nanotubes for Improving the Mechanical and Electrical Properties of Oil-Well Cement-Based Composites. *ACS Appl. Nano Mater.* **2022**, *5* (5), 6671–6678. https://doi.org/10.1021/acsanm.2c00706.

(21) Price, G. J.; Nawaz, M.; Yasin, T.; Bibi, S. Sonochemical Modification of Carbon Nanotubes for Enhanced Nanocomposite Performance. *Ultrasonics Sonochemistry* **2018**, *40*, 123–130. https://doi.org/10.1016/j.ultsonch.2017.02.021.

(22) Weight, B. M.; Gifford, B. J.; Tiffany, G.; Henderson, E.; Mihaylov, D.; Kilin, D.; Kilina, S. Optically Active Defects in Carbon Nanotubes *via* Chlorination: Computational Insights. *RSC Appl. Interfaces* **2024**, *1* (2), 281–300. https://doi.org/10.1039/D3LF00064H.

(23) Dementjev, A. P.; Eletskii, A. V.; Maslakov, K. I.; Rakov, E. G.; Sukhoverhov, V. F.; Naumkin, A. V. Fluorination of Carbon Nanostructures and Their Comparative Investigation by XPS and XAES Spectroscopy. *Fullerenes, Nanotubes and Carbon Nanostructures* **2006**, *14* (2–3), 287–296. https://doi.org/10.1080/15363830600663990.

(24) Li, D.; Luo, Y.; Onidas, D.; He, L.; Jin, M.; Gazeau, F.; Pinson, J.; Mangeney, C. Surface Functionalization of Nanomaterials by Aryl Diazonium Salts for Biomedical Sciences. *Advances in Colloid and Interface Science* **2021**, *294*, 102479. https://doi.org/10.1016/j.cis.2021.102479.

(25) Morales-Lara, F.; Domingo-García, M.; López-Garzón, R.; Luz Godino-Salido, M.; Peñas-Sanjuán, A.; López-Garzón, F. J.; Pérez-Mendoza, M.; Melguizo, M. Grafting the Surface of Carbon Nanotubes and Carbon Black with the Chemical Properties of Hyperbranched Polyamines. *Science and Technology of Advanced Materials* **2016**, *17* (1), 541–553. https://doi.org/10.1080/14686996.2016.1221728.

(26) Madikere Raghunatha Reddy, A. K.; Darwiche, A.; Reddy, M. V.; Zaghib, K. Review on Advancements in Carbon Nanotubes: Synthesis, Purification, and Multifaceted Applications. *Batteries* **2025**, *11* (2), 71. https://doi.org/10.3390/batteries11020071.

(27) Rennhofer, H.; Zanghellini, B. Dispersion State and Damage of Carbon Nanotubes and Carbon Nanofibers by Ultrasonic Dispersion: A Review. *Nanomaterials* **2021**, *11* (6), 1469. https://doi.org/10.3390/nano11061469.

(28) Yu, W.; Sisi, L.; Haiyan, Y.; Jie, L. Progress in the Functional Modification of Graphene/Graphene Oxide: A Review. *RSC Adv.* **2020**, *10* (26), 15328–15345. https://doi.org/10.1039/D0RA01068E.

(29) Choi, W.; Lahiri, I.; Seelaboyina, R.; Kang, Y. S. Synthesis of Graphene and Its Applications: A Review. *Critical Reviews in Solid State and Materials Sciences* **2010**, *35* (1), 52–71. https://doi.org/10.1080/10408430903505036.

(30) ISO-TS-80004-13-2017.

(31) Lee, H. C.; Liu, W.-W.; Chai, S.-P.; Mohamed, A. R.; Lai, C. W.; Khe, C.-S.; Voon, C. H.; Hashim, U.; Hidayah, N. M. S. Synthesis of Single-Layer Graphene: A Review of Recent Development. *Procedia Chemistry* **2016**, *19*, 916–921. https://doi.org/10.1016/j.proche.2016.03.135.

(32) Lee, C.; Wei, X.; Kysar, J. W.; Hone, J. Measurement of the Elastic Properties and Intrinsic Strength of Monolayer Graphene. *Science* **2008**, *321* (5887), 385–388. https://doi.org/10.1126/science.1157996.

(33) Nair, R. R.; Blake, P.; Grigorenko, A. N.; Novoselov, K. S.; Booth, T. J.; Stauber, T.; Peres, N. M. R.; Geim, A. K. Fine Structure Constant Defines Visual Transparency of Graphene. *Science* **2008**, *320* (5881), 1308–1308. https://doi.org/10.1126/science.1156965.

(34) Lim, S.; Park, H.; Yamamoto, G.; Lee, C.; Suk, J. W. Measurements of the Electrical Conductivity of Monolayer Graphene Flakes Using Conductive Atomic Force Microscopy. *Nanomaterials* **2021**, *11* (10), 2575. https://doi.org/10.3390/nano11102575.

(35) Ramezani, M.; Alibolandi, M.; Nejabat, M.; Charbgoo, F.; Taghdisi, S. M.; Abnous, K. Graphene-Based Hybrid Nanomaterials for Biomedical Applications. In *Biomedical Applications of Graphene and 2D Nanomaterials*; Elsevier, 2019; pp 119–141. https://doi.org/10.1016/B978-0-12-815889-0.00006-4.

(36) Sonia, F. J.; Aslam, M.; Mukhopadhyay, A. Understanding the Processing-Structure-Performance Relationship of Graphene and Its Variants as Anode Material for Li-Ion Batteries: A Critical Review. *Carbon* **2020**, *156*, 130–165. https://doi.org/10.1016/j.carbon.2019.09.026.

(37) Celis, A.; Nair, M. N.; Taleb-Ibrahimi, A.; Conrad, E. H.; Berger, C.; De Heer, W. A.; Tejeda, A. Graphene Nanoribbons: Fabrication, Properties and Devices. *J. Phys. D: Appl. Phys.* **2016**, *49* (14), 143001. https://doi.org/10.1088/0022-3727/49/14/143001.

(38) Jiříčková, A.; Jankovský, O.; Sofer, Z.; Sedmidubský, D. Synthesis and Applications of Graphene Oxide. *Materials* **2022**, *15* (3), 920. https://doi.org/10.3390/ma15030920.

(39) Tarcan, R.; Todor-Boer, O.; Petrovai, I.; Leordean, C.; Astilean, S.; Botiz, I. Reduced Graphene Oxide Today. *J. Mater. Chem. C* **2020**, *8* (4), 1198–1224. https://doi.org/10.1039/C9TC04916A.

(40) George, M.; Jose, R.; Anju, T. R. Bottom Up Approaches in Nanomaterial Synthesis. In *Nanomaterial Green Synthesis*; Al-Khayri, J. M., Anju, T. R., Jain, S. M., Eds.; Nanotechnology in Plant Sciences; Springer Nature Switzerland: Cham, 2025; Vol. 2, pp 453–481. https://doi.org/10.1007/978-3-031-84643-4_15.

(41) Wang, X.-D.; Vinodgopal, K.; Dai, G.-P. Synthesis of Carbon Nanotubes by Catalytic Chemical Vapor Deposition. In *Perspective of Carbon Nanotubes*; El-Din Saleh, H., Moawad Mohamed El-Sheikh, S., Eds.; IntechOpen, 2019. https://doi.org/10.5772/intechopen.86995.

(42) Journet, C.; Maser, W. K.; Bernier, P.; Loiseau, A.; De La Chapelle, M. L.; Lefrant, S.; Deniard, P.; Lee, R.; Fischer, J. E. Large-Scale Production of Single-Walled Carbon Nanotubes by the Electric-Arc Technique. *Nature* **1997**, *388* (6644), 756–758. https://doi.org/10.1038/41972.

(43) Guo, T.; Nikolaev, P.; Thess, A.; Colbert, D. T.; Smalley, R. E. Catalytic Growth of Single-Walled Nanotubes by Laser Vaporization. *Chemical Physics Letters* **1995**, *243* (1–2), 49–54. https://doi.org/10.1016/0009-2614(95)00825-O.

(44) Yazdi, G.; Iakimov, T.; Yakimova, R. Epitaxial Graphene on SiC: A Review of Growth and Characterization. *Crystals* **2016**, *6* (5), 53. https://doi.org/10.3390/cryst6050053.

(45) Khan, F. A. Synthesis of Nanomaterials: Methods & Technology. In *Applications of Nanomaterials in Human Health*; Khan, F. A., Ed.; Springer Singapore: Singapore, 2020; pp 15–21. https://doi.org/10.1007/978-981-15-4802-4_2.

(46) Novoselov, K. S.; Geim, A. K.; Morozov, S. V.; Jiang, D.; Zhang, Y.; Dubonos, S. V.; Grigorieva, I. V.; Firsov, A. A. Electric Field Effect in Atomically Thin Carbon Films. *Science* **2004**, *306* (5696), 666–669. https://doi.org/10.1126/science.1102896.

(47) Gebreegziabher, G. G.; Asemahegne, A. S.; Ayele, D. W.; Dhakshnamoorthy, M.; Kumar, A. One-Step Synthesis and Characterization of Reduced Graphene Oxide Using Chemical Exfoliation Method. *Materials Today Chemistry* **2019**, *12*, 233–239. https://doi.org/10.1016/j.mtchem.2019.02.003.

(48) Casallas Caicedo, F. M.; Vera López, E.; Agarwal, A.; Drozd, V.; Durygin, A.; Franco Hernandez, A.; Wang, C. Synthesis of Graphene Oxide from Graphite by Ball Milling. *Diamond and Related Materials* **2020**, *109*, 108064. https://doi.org/10.1016/j.diamond.2020.108064.

(49) Sommer, B.; Sonntag, J.; Ganczarczyk, A.; Braam, D.; Prinz, G.; Lorke, A.; Geller, M. Electron-Beam Induced Nano-Etching of Suspended Graphene. *Sci Rep* **2015**, *5* (1), 7781. https://doi.org/10.1038/srep07781.

(50) Pant, M.; Singh, R.; Negi, P.; Tiwari, K.; Singh, Y. A Comprehensive Review on Carbon Nano-Tube Synthesis Using Chemical Vapor Deposition. *Materials Today: Proceedings* **2021**, *46*, 11250–11253. https://doi.org/10.1016/j.matpr.2021.02.646.

(51) Chiang, H.-L.; Wu, F.-Y.; Huang, P.-H.; Lee, T.-Y. Characteristics of Acetylene Cracking on MCM-41 to Form Carbon Materials and Their Exhaust Emission. *Microporous and Mesoporous Materials* **2018**, *268*, 100–108. https://doi.org/10.1016/j.micromeso.2018.04.006.

(52) Hussain, A.; Liao, Y.; Zhang, Q.; Ding, E.-X.; Laiho, P.; Ahmad, S.; Wei, N.; Tian, Y.; Jiang, H.; Kauppinen, E. I. Floating Catalyst CVD Synthesis of Single Walled Carbon Nanotubes from Ethylene for High Performance Transparent Electrodes. *Nanoscale* **2018**, *10* (20), 9752–9759. https://doi.org/10.1039/C8NR00716K.

(53) Boncel, S.; Jędrysiak, R. G.; Czerw, M.; Kolanowska, A.; Blacha, A. W.; Imielski, M.; Jóźwiak, B.; Dzida, M. H.; Greer, H. F.; Sobotnicki, A. Paintable Carbon Nanotube Coating-Based Textronics for Sustained Holter-Type Electrocardiography. *ACS Appl. Nano Mater.* **2022**, *5* (10), 15762–15774. https://doi.org/10.1021/acsanm.2c03904.

(54) Chopra, N.; Hinds, B. Catalytic Size Control of Multiwalled Carbon Nanotube Diameter in Xylene Chemical Vapor Deposition Process. *Inorganica Chimica Acta* **2004**, *357* (13), 3920–3926. https://doi.org/10.1016/j.ica.2004.08.022.

(55) Gj, M. Synthesis of Carbon Nanotubes Using Aliphatic Alcohols as a Carbon Source. *Chem Sci J* **2015**, *6* (3). https://doi.org/10.4172/2150-3494.1000e110.

(56) Sinnott, S. B.; Andrews, R. Carbon Nanotubes: Synthesis, Properties, and Applications. *Critical Reviews in Solid State and Materials Sciences* **2001**, *26* (3), 145–249. https://doi.org/10.1080/20014091104189.

(57) Ando, Y.; Zhao, X.; Sugai, T.; Kumar, M. Growing Carbon Nanotubes. *Materials Today* **2004**, *7* (10), 22–29. https://doi.org/10.1016/S1369-7021(04)00446-8.

(58) Zhao, X.; Chu, D.; Zhang, X.; Gao, C.; He, Y.; Bai, W. Growth and Characterization of Carbon Nanotubes and Study of Modified Carbon Fiber—A Review. *Diamond and Related Materials* **2024**, *147*, 111308. https://doi.org/10.1016/j.diamond.2024.111308.

(59) Danafar, F.; Fakhru'l-Razi, A.; Salleh, M. A. M.; Biak, D. R. A. Fluidized Bed Catalytic Chemical Vapor Deposition Synthesis of Carbon Nanotubes—A Review. *Chemical Engineering Journal* **2009**, *155* (1–2), 37–48. https://doi.org/10.1016/j.cej.2009.07.052.

(60) Dasgupta, K.; Joshi, J. B.; Banerjee, S. Fluidized Bed Synthesis of Carbon Nanotubes – A Review. *Chemical Engineering Journal* **2011**, *171* (3), 841–869. https://doi.org/10.1016/j.cej.2011.05.038.

(61) Franz, G. Plasma Enhanced Chemical Vapor Deposition of Organic Polymers. *Processes* **2021**, *9* (6), 980. https://doi.org/10.3390/pr9060980.

(62) Chaisitsak, S.; Yamada, A.; Konagai, M. Hot Filament Enhanced CVD Synthesis of Carbon Nanotubes by Using a Carbon Filament. *Diamond and Related Materials* **2004**, *13* (3), 438–444. https://doi.org/10.1016/S0925-9635(03)00572-7.

(63) Yabe, Y.; Ohtake, Y.; Ishitobi, T.; Show, Y.; Izumi, T.; Yamauchi, H. Synthesis of Well-Aligned Carbon Nanotubes by Radio Frequency Plasma Enhanced CVD Method. *Diamond and Related Materials* **2004**, *13* (4–8), 1292–1295. https://doi.org/10.1016/j.diamond.2003.11.067.

(64) Liu, Y.; He, J.; Zhang, N.; Zhang, W.; Zhou, Y.; Huang, K. Advances of Microwave Plasma-Enhanced Chemical Vapor Deposition in Fabrication of Carbon Nanotubes: A Review. *J Mater Sci* **2021**, *56* (22), 12559–12583. https://doi.org/10.1007/s10853-021-06128-1.

(65) Acharya, S.; Alexender, R.; Sahu, A. K.; Nechiyil, D.; Verma, A.; Kaushal, A.; Prakash, J.; Dasgupta, K. Water Assisted Atmospheric CVD Super Growth of Vertically Aligned CNT Forest for Supercapacitor Application. *Diamond and Related Materials* **2024**, *148*, 111481. https://doi.org/10.1016/j.diamond.2024.111481.

(66) Sato, T.; Sugime, H.; Noda, S. CO2-Assisted Growth of Millimeter-Tall Single-Wall Carbon Nanotube Arrays and Its Advantage against H2O for Large-Scale and Uniform Synthesis. *Carbon* **2018**, *136*, 143–149. https://doi.org/10.1016/j.carbon.2018.04.060.

(67) Zhang, Y.; Liao, M. X.; Deng, S. Z.; Chen, J.; Xu, N. S. In Situ Oxygen-Assisted Field Emission Treatment for Improving the Uniformity of Carbon Nanotube Pixel Arrays and the Underlying Mechanism. *Carbon* **2011**, *49* (10), 3299–3306. https://doi.org/10.1016/j.carbon.2011.04.006.

(68) Li, Y.; Xu, G.; Zhang, H.; Li, T.; Yao, Y.; Li, Q.; Dai, Z. Alcohol-Assisted Rapid Growth of Vertically Aligned Carbon Nanotube Arrays. *Carbon* **2015**, *91*, 45–55. https://doi.org/10.1016/j.carbon.2015.04.035.

(69) Lim, J.-V.; Bee, S.-T.; Tin Sin, L.; Ratnam, C. T.; Abdul Hamid, Z. A. A Review on the Synthesis, Properties, and Utilities of Functionalized Carbon Nanoparticles for Polymer Nanocomposites. *Polymers* **2021**, *13* (20), 3547. https://doi.org/10.3390/polym13203547.

(70) Dutta, S. D.; Patel, D. K.; Lim, K.-T. Carbon Nanotube-Based Nanohybrids for Agricultural and Biological Applications. In *Multifunctional Hybrid Nanomaterials for Sustainable Agri-Food and Ecosystems*; Elsevier, 2020; pp 505–535. https://doi.org/10.1016/B978-0-12-821354-4.00021-2.

(71) Xu, S.; Zhang, L.; Wang, B.; Ruoff, R. S. Chemical Vapor Deposition of Graphene on Thin-Metal Films. *Cell Reports Physical Science* **2021**, *2* (3), 100372. https://doi.org/10.1016/j.xcrp.2021.100372.

(72) Saeed, M.; Alshammari, Y.; Majeed, S. A.; Al-Nasrallah, E. Chemical Vapour Deposition of Graphene—Synthesis, Characterisation, and Applications: A Review. *Molecules* **2020**, *25* (17), 3856. https://doi.org/10.3390/molecules25173856.

(73) Convertino, D.; Trincavelli, M. L.; Giacomelli, C.; Marchetti, L.; Coletti, C. Graphene-Based Nanomaterials for Peripheral Nerve Regeneration. *Front. Bioeng. Biotechnol.* **2023**, *11*, 1306184. https://doi.org/10.3389/fbioe.2023.1306184.

(74) Garg, R.; Dutta, N.; Choudhury, N. Work Function Engineering of Graphene. *Nanomaterials* **2014**, *4* (2), 267–300. https://doi.org/10.3390/nano4020267.

(75) Ghosh, P.; Afre, R. A.; Soga, T.; Jimbo, T. A Simple Method of Producing Single-Walled Carbon Nanotubes from a Natural Precursor: Eucalyptus Oil. *Materials Letters* **2007**, *61* (17), 3768–3770. https://doi.org/10.1016/j.matlet.2006.12.030.

(76) Alhajri, H. M.; Aloqaili, S. S.; Alterary, S. S.; Alqathama, A.; Abdalla, A. N.; Alzhrani, R. M.; Alotaibi, B. S.; Alsaab, H. O. Olive Leaf Extracts for a Green Synthesis of Silver-Functionalized Multi-Walled Carbon Nanotubes. *JFB* **2022**, *13* (4), 224. https://doi.org/10.3390/jfb13040224.

(77) Kang, Z.; Wang, E.; Mao, B.; Su, Z.; Chen, L.; Xu, L. Obtaining Carbon Nanotubes from Grass. *Nanotechnology* **2005**, *16* (8), 1192–1195. https://doi.org/10.1088/0957-4484/16/8/036.

(78) Janas, D. From Bio to Nano: A Review of Sustainable Methods of Synthesis of Carbon Nanotubes. *Sustainability* **2020**, *12* (10), 4115. https://doi.org/10.3390/su12104115.

(79) Dipta, I. K. R. A.; Lee, C. W. Recent Advances and Perspectives in Carbon Nanotube Production from the Electrochemical Conversion of Carbon Dioxide. *Journal of CO2 Utilization* **2024**, *82*, 102745. https://doi.org/10.1016/j.jcou.2024.102745.

(80) Eatemadi, A.; Daraee, H.; Karimkhanloo, H.; Kouhi, M.; Zarghami, N.; Akbarzadeh, A.; Abasi, M.; Hanifehpour, Y.; Joo, S. W. Carbon Nanotubes: Properties, Synthesis, Purification, and Medical Applications. *Nanoscale Res Lett* **2014**, *9* (1), 393. https://doi.org/10.1186/1556-276X-9-393.

(81) Yu, M.-F.; Lourie, O.; Dyer, M. J.; Moloni, K.; Kelly, T. F.; Ruoff, R. S. Strength and Breaking Mechanism of Multiwalled Carbon Nanotubes Under Tensile Load. *Science* **2000**, *287* (5453), 637–640. https://doi.org/10.1126/science.287.5453.637.

(82) Pavlina, E. J.; Van Tyne, C. J. Correlation of Yield Strength and Tensile Strength with Hardness for Steels. *J. of Materi Eng and Perform* **2008**, *17* (6), 888–893. https://doi.org/10.1007/s11665-008-9225-5.

(83) Cao, K.; Feng, S.; Han, Y.; Gao, L.; Hue Ly, T.; Xu, Z.; Lu, Y. Elastic Straining of Free-Standing Monolayer Graphene. *Nat Commun* **2020**, *11* (1), 284. https://doi.org/10.1038/s41467-019-14130-0.

(84) Bai, Y.; Yue, H.; Zhang, R.; Qian, W.; Zhang, Z.; Wei, F. Mechanical Behavior of Single and Bundled Defect-Free Carbon Nanotubes. *Acc. Mater. Res.* **2021**, *2* (11), 998–1009. https://doi.org/10.1021/accountsmr.1c00120.

(85) Nurazzi, N. M.; Sabaruddin, F. A.; Harussani, M. M.; Kamarudin, S. H.; Rayung, M.; Asyraf, M. R. M.; Aisyah, H. A.; Norrrahim, M. N. F.; Ilyas, R. A.; Abdullah, N.; Zainudin, E. S.; Sapuan, S. M.; Khalina, A. Mechanical Performance and Applications of CNTs Reinforced Polymer Composites—A Review. *Nanomaterials* **2021**, *11* (9), 2186. https://doi.org/10.3390/nano11092186.

(86) Lamnini, S.; Pugliese, D.; Baino, F. Zirconia-Based Ceramics Reinforced by Carbon Nanotubes: A Review with Emphasis on Mechanical Properties. *Ceramics* **2023**, *6* (3), 1705–1734. https://doi.org/10.3390/ceramics6030105.

(87) Curtin, W. A.; Sheldon, B. W. CNT-Reinforced Ceramics and Metals. *Materials Today* **2004**, *7* (11), 44–49. https://doi.org/10.1016/S1369-7021(04)00508-5.

(88) Kiran, M. D.; Govindaraju, H. K.; Kumar, N.; Nagaral, M.; Khankal, D. V.; Pandhare, A. P.; Babu, E. R.; Anjinappa, C.; Razak, A.; Wodajo, A. W. Effect of CNT Filler and Temperature on Fracture Toughness of Epoxy Composites Reinforced with Carbon Fabric. *Engineering Reports* **2024**, *6* (8), e12816. https://doi.org/10.1002/eng2.12816.

(89) Dericiler, K.; Aliyeva, N.; Mohammadjafari Sadeghi, H.; Sas, H. S.; Menceloglu, Y. Z.; Saner Okan, B. Graphene in Automotive Parts. In *Nanotechnology in the Automotive Industry*; Elsevier, 2022; pp 623–651. https://doi.org/10.1016/B978-0-323-90524-4.00030-X.

(90) Kausar, A.; Rafique, I.; Muhammad, B. Aerospace Application of Polymer Nanocomposite with Carbon Nanotube, Graphite, Graphene Oxide, and Nanoclay. *Polymer-Plastics Technology and Engineering* **2017**, *56* (13), 1438–1456. https://doi.org/10.1080/03602559.2016.1276594.

(91) Sinha, A.; Behera, A. Nanotechnology in the Space Industry. In *Nanotechnology-Based Smart Remote Sensing Networks for Disaster Prevention*; Elsevier, 2022; pp 139–157. https://doi.org/10.1016/B978-0-323-91166-5.00005-7.

(92) Singh, S.; Kumar, A.; Kamboj, M.; Das, B.; Singh, H.; Rakha, K. Scratch Resistance and In-Vitro Biocompatibility of Plasma-Sprayed Baghdadite Coatings Reinforced with Carbon Nanotubes. *Surface and Coatings Technology* **2024**, *481*, 130670. https://doi.org/10.1016/j.surfcoat.2024.130670.

(93) Laurenzi, S.; Pastore, R.; Giannini, G.; Marchetti, M. Experimental Study of Impact Resistance in Multi-Walled Carbon Nanotube Reinforced Epoxy. *Composite Structures* **2013**, *99*, 62–68. https://doi.org/10.1016/j.compstruct.2012.12.002.

(94) Wang, X.; Qi, X.; Lin, Z.; Battocchi, D. Graphene Reinforced Composites as Protective Coatings for Oil and Gas Pipelines. *Nanomaterials* **2018**, *8* (12), 1005. https://doi.org/10.3390/nano8121005.

(95) Kim, H.-S.; Kang, J.-H.; Hwang, J.-Y.; Shin, U. S. Wearable CNTs-Based Humidity Sensors with High Sensitivity and Flexibility for Real-Time Multiple Respiratory Monitoring. *Nano Convergence* **2022**, *9* (1), 35. https://doi.org/10.1186/s40580-022-00326-6.

(96) Https://Publishing.Aip.Org/Publications/Latest-Content/Improving-High-Energy-Lithium-Ion-Batteries-with-Carbon-Filler/.

(97) Esteghamat, A.; Akhavan, O. Graphene as the Ultra-Transparent Conductive Layer in Developing the Nanotechnology-Based Flexible Smart Touchscreens. *Microelectronic Engineering* **2023**, *267–268*, 111899. https://doi.org/10.1016/j.mee.2022.111899.

(98) Novoselov, K. S.; Fal′ko, V. I.; Colombo, L.; Gellert, P. R.; Schwab, M. G.; Kim, K. A Roadmap for Graphene. *Nature* **2012**, *490* (7419), 192–200. https://doi.org/10.1038/nature11458.

(99) Sarma, S. D.; Adam, S.; Hwang, E. H.; Rossi, E. Electronic Transport in Two Dimensional Graphene. **2010**. https://doi.org/10.48550/ARXIV.1003.4731.

(100) Zhu, S.; Sheng, J.; Chen, Y.; Ni, J.; Li, Y. Carbon Nanotubes for Flexible Batteries: Recent Progress and Future Perspective. *National Science Review* **2021**, *8* (5), nwaa261. https://doi.org/10.1093/nsr/nwaa261.

(101) Yao, X.; Zhang, Y.; Jin, W.; Hu, Y.; Cui, Y. Carbon Nanotube Field-Effect Transistor-Based Chemical and Biological Sensors. *Sensors* **2021**, *21* (3), 995. https://doi.org/10.3390/s21030995.

(102) Díez-Pascual, A. M.; Rahdar, A. Graphene-Based Polymer Composites for Flexible Electronic Applications. *Micromachines* **2022**, *13* (7), 1123. https://doi.org/10.3390/mi13071123.

(103) Liao, L.; Duan, X. Graphene for Radio Frequency Electronics. *Materials Today* **2012**, *15* (7–8), 328–338. https://doi.org/10.1016/S1369-7021(12)70138-4.

(104) Meyyappan, M. Carbon Nanotube-Based Chemical Sensors. *Small* **2016**, *12* (16), 2118–2129. https://doi.org/10.1002/smll.201502555.

(105) Zhu, Z. An Overview of Carbon Nanotubes and Graphene for Biosensing Applications. *Nano-Micro Lett.* **2017**, *9* (3), 25. https://doi.org/10.1007/s40820-017-0128-6.

(106) Jain, P.; Rajput, R. S.; Kumar, S.; Sharma, A.; Jain, A.; Bora, B. J.; Sharma, P.; Kumar, R.; Shahid, M.; Rajhi, A. A.; Alsubih, M.; Shah, M. A.; Bhowmik, A. Recent Advances in Graphene-Enabled Materials for Photovoltaic Applications: A Comprehensive Review. *ACS Omega* **2024**, acsomega.3c07994. https://doi.org/10.1021/acsomega.3c07994.

(107) Esteghamat, A.; Akhavan, O. Graphene as the Ultra-Transparent Conductive Layer in Developing the Nanotechnology-Based Flexible Smart Touchscreens. *Microelectronic Engineering* **2023**, *267–268*, 111899. https://doi.org/10.1016/j.mee.2022.111899.

(108) Yuan, W.; Zhang, Y.; Cheng, L.; Wu, H.; Zheng, L.; Zhao, D. The Applications of Carbon Nanotubes and Graphene in Advanced Rechargeable Lithium Batteries. *J. Mater. Chem. A* **2016**, *4* (23), 8932–8951. https://doi.org/10.1039/C6TA01546H.

(109) Pour, G. B.; Ashourifar, H.; Aval, L. F.; Solaymani, S. CNTs-Supercapacitors: A Review of Electrode Nanocomposites Based on CNTs, Graphene, Metals, and Polymers. *Symmetry* **2023**, *15* (6), 1179. https://doi.org/10.3390/sym15061179.

(110) Chen, L.; Chen, S.; Hou, Y. Understanding the Thermal Conductivity of Diamond/Copper Composites by First-Principles Calculations. *Carbon* **2019**, *148*, 249–257. https://doi.org/10.1016/j.carbon.2019.03.051.

(111)Pop, E.; Mann, D.; Wang, Q.; Goodson, K.; Dai, H. Thermal Conductance of an Individual Single-Wall Carbon Nanotube above Room Temperature. *Nano Lett.* **2006**, *6* (1), 96–100. https://doi.org/10.1021/nl052145f.

(112) Han, Z.; Fina, A. Thermal Conductivity of Carbon Nanotubes and Their Polymer Nanocomposites: A Review. *Progress in Polymer Science* **2011**, *36* (7), 914–944. https://doi.org/10.1016/j.progpolymsci.2010.11.004.

(113) Kwon, Y.-K.; Kim, P. Unusually High Thermal Conductivity in Carbon Nanotubes. In *High Thermal Conductivity Materials*; Shindé, S. L., Goela, J. S., Eds.; Springer-Verlag: New York, 2006; pp 227–265. https://doi.org/10.1007/0-387-25100-6_8.

(114) Das, H. Thermal Transport in Multi-Walled Carbon Nanotubes. *Res. Rev. J Mat. Sci* **2017**, *05* (03). https://doi.org/10.4172/2321-6212.1000176.

(115) Balandin, A. A.; Ghosh, S.; Bao, W.; Calizo, I.; Teweldebrhan, D.; Miao, F.; Lau, C. N. Superior Thermal Conductivity of Single-Layer Graphene. *Nano Lett.* **2008**, *8* (3), 902–907. https://doi.org/10.1021/nl0731872.

(116) Amani, M.; Burke, R. A.; Proie, R. M.; Dubey, M. Flexible Integrated Circuits and Multifunctional Electronics Based on Single Atomic Layers of MoS_2 and Graphene. *Nanotechnology* **2015**, *26* (11), 115202. https://doi.org/10.1088/0957-4484/26/11/115202.

(117) Yan, Z.; Liu, G.; Khan, J. M.; Balandin, A. A. Graphene Quilts for Thermal Management of High-Power GaN Transistors. *Nat Commun* **2012**, *3* (1), 827. https://doi.org/10.1038/ncomms1828.

(118) Han, N.; Viet Cuong, T.; Han, M.; Deul Ryu, B.; Chandramohan, S.; Bae Park, J.; Hye Kang, J.; Park, Y.-J.; Bok Ko, K.; Yun Kim, H.; Kyu Kim, H.; Hyoung Ryu, J.; Katharria, Y. S.; Choi, C.-J.; Hong, C.-H. Improved Heat Dissipation in Gallium Nitride Light-Emitting Diodes with Embedded Graphene Oxide Pattern. *Nat Commun* **2013**, *4* (1), 1452. https://doi.org/10.1038/ncomms2448.

(119) Li, A.; Zhang, C.; Zhang, Y.-F. Thermal Conductivity of Graphene-Polymer Composites: Mechanisms, Properties, and Applications. *Polymers* **2017**, *9* (9), 437. https://doi.org/10.3390/polym9090437.

(120) Tran, T. Q.; Deshpande, S.; Dasari, S. S.; Arole, K.; Johnson, D.; Zhang, Y.; Harkin, E. M.; Djire, A.; Seet, H. L.; Nai, S. M. L.; Green, M. J. 3D Printed Carbon Nanotube/Phenolic Composites for Thermal Dissipation and Electromagnetic Interference Shielding. *ACS Appl. Mater. Interfaces* **2024**, *16* (50), 69929–69939. https://doi.org/10.1021/acsami.4c17115.

(121) Zhu, Q.; Ong, P. J.; Goh, S. H. A.; Yeo, R. J.; Wang, S.; Liu, Z.; Loh, X. J. Recent Advances in Graphene-Based Phase Change Composites for Thermal Energy Storage and Management. *Nano Materials Science* **2024**, *6* (2), 115–138. https://doi.org/10.1016/j.nanoms.2023.09.003.

(122) Said, Z.; Pandey, A. K.; Tiwari, A. K.; Kalidasan, B.; Jamil, F.; Thakur, A. K.; Tyagi, V. V.; Sarı, A.; Ali, H. M. Nano-Enhanced Phase Change Materials: Fundamentals and Applications. *Progress in Energy and Combustion Science* **2024**, *104*, 101162. https://doi.org/10.1016/j.pecs.2024.101162.

(123) Janas, D.; Rdest, M.; Koziol, K. K. K. Flame-Retardant Carbon Nanotube Films. *Applied Surface Science* **2017**, *411*, 177–181. https://doi.org/10.1016/j.apsusc.2017.03.144.

(124) Blaikie, A.; Miller, D.; Alemán, B. J. A Fast and Sensitive Room-Temperature Graphene Nanomechanical Bolometer. *Nat Commun* **2019**, *10* (1), 4726. https://doi.org/10.1038/s41467-019-12562-2.

(125) Vertuccio, L.; De Santis, F.; Pantani, R.; Lafdi, K.; Guadagno, L. Effective De-Icing Skin Using Graphene-Based Flexible Heater. *Composites Part B: Engineering* **2019**, *162*, 600–610. https://doi.org/10.1016/j.compositesb.2019.01.045.

(126) Sequino, L.; Sebastianelli, G.; Vaglieco, B. M. Carbon and Graphene Coatings for the Thermal Management of Sustainable LMP Batteries for Automotive Applications. *Materials* **2022**, *15* (21), 7744. https://doi.org/10.3390/ma15217744.

(127) Zhao, H.-Y.; Yu, M.-Y.; Liu, J.; Li, X.; Min, P.; Yu, Z.-Z. Efficient Preconstruction of Three-Dimensional Graphene Networks for Thermally Conductive Polymer Composites. *Nano-Micro Lett.* **2022**, *14* (1), 129. https://doi.org/10.1007/s40820-022-00878-6.

(128) Charlier, J.-C.; Blase, X.; Roche, S. Electronic and Transport Properties of Nanotubes. *Rev. Mod. Phys.* **2007**, *79* (2), 677–732. https://doi.org/10.1103/RevModPhys.79.677.

(129) Balandin, A. A. Thermal Properties of Graphene and Nanostructured Carbon Materials. *Nature Mater* **2011**, *10* (8), 569–581. https://doi.org/10.1038/nmat3064.

(130) Yang, G.; Li, L.; Lee, W. B.; Ng, M. C. Structure of Graphene and Its Disorders: A Review. *Science and Technology of Advanced Materials* **2018**, *19* (1), 613–648. https://doi.org/10.1080/14686996.2018.1494493.

(131) Bauhofer, W.; Kovacs, J. Z. A Review and Analysis of Electrical Percolation in Carbon Nanotube Polymer Composites. *Composites Science and Technology* **2009**, *69* (10), 1486–1498. https://doi.org/10.1016/j.compscitech.2008.06.018.

(132) Khan, T.; Irfan, M. S.; Ali, M.; Dong, Y.; Ramakrishna, S.; Umer, R. Insights to Low Electrical Percolation Thresholds of Carbon-Based Polypropylene Nanocomposites. *Carbon* **2021**, *176*, 602–631. https://doi.org/10.1016/j.carbon.2021.01.158.

(133) Hassan, E. A. M.; Yang, L.; Elagib, T. H. H.; Ge, D.; Lv, X.; Zhou, J.; Yu, M.; Zhu, S. Synergistic Effect of Hydrogen Bonding and π-π Stacking in Interface of CF/PEEK Composites. *Composites Part B: Engineering* **2019**, *171*, 70–77. https://doi.org/10.1016/j.compositesb.2019.04.015.

(134) Yuan, H.; Han, S.; Wei, J.; Li, S.; Yang, P.; Mi, H.-Y.; Liu, C.; Shen, C. Noncovalent Cross-Linked Engineering Hydrogel with Low Hysteresis and High Sensitivity for Flexible Self-Powered Electronics. *Journal of Energy Chemistry* **2024**, *94*, 136–147. https://doi.org/10.1016/j.jechem.2024.02.039.

(135) Qian, D. Load Transfer Mechanism in Carbon Nanotube Ropes. *Composites Science and Technology* **2003**, *63* (11), 1561–1569. https://doi.org/10.1016/S0266-3538(03)00064-2.

(136) Park, J. S.; Park, J. Y.; Kim, J. S.; Kang, Y.; Kim, S. M.; Song, K. S.; Kim, H. W.; Park, Y. J.; Kim, G.; Song, K.; Lee, S.; Yun, D.; Cho, Y. S.; Yang, S. J. Molecular-Level Network Engineering of Crosslinker towards High-Performance Carbon Nanotube Fiber. *Composites Part B: Engineering* **2024**, *275*, 111338. https://doi.org/10.1016/j.compositesb.2024.111338.

(137) Rao, C. N. R.; Pramoda, K.; Kumar, R. Covalent Cross-Linking as a Strategy to Generate Novel Materials Based on Layered (2D) and Other Low D Structures. *Chem. Commun.* **2017**, *53* (73), 10093–10107. https://doi.org/10.1039/C7CC05390H.

(138) Xie, Y.; Wang, X.; Hou, L.; Wang, X.; Zhang, Y.; Zhu, C.; Hu, Z.; He, M. Graphene Covalently Functionalized by Cross-Linking Reaction of Bifunctional Pillar Organic Molecule for High Capacitance. *Journal of Energy Storage* **2021**, *38*, 102530. https://doi.org/10.1016/j.est.2021.102530.

(139) Chandler, D. Interfaces and the Driving Force of Hydrophobic Assembly. *Nature* **2005**, *437* (7059), 640–647. https://doi.org/10.1038/nature04162.

(140) Gao, C.; Guo, M.; Liu, Y.; Zhang, D.; Gao, F.; Sun, L.; Li, J.; Chen, X.; Terrones, M.; Wang, Y. Surface Modification Methods and Mechanisms in Carbon Nanotubes Dispersion. *Carbon* **2023**, *212*, 118133. https://doi.org/10.1016/j.carbon.2023.118133.

(141) Haar, S.; El Gemayel, M.; Shin, Y.; Melinte, G.; Squillaci, M. A.; Ersen, O.; Casiraghi, C.; Ciesielski, A.; Samorì, P. Enhancing the Liquid-Phase Exfoliation of Graphene in Organic Solvents upon Addition of n-Octylbenzene. *Sci Rep* **2015**, *5* (1), 16684. https://doi.org/10.1038/srep16684.

(142) Belyaeva, L. A.; Van Deursen, P. M. G.; Barbetsea, K. I.; Schneider, G. F. Hydrophilicity of Graphene in Water through Transparency to Polar and Dispersive Interactions. *Advanced Materials* **2018**, *30* (6), 1703274. https://doi.org/10.1002/adma.201703274.

(143) Loponov, K. N.; Deadman, B. J.; Zhu, J.; Rielly, C.; Holdich, R. G.; Hii, K. K. (Mimi); Hellgardt, K. Controlled Multiphase Oxidations for Continuous Manufacturing of Fine Chemicals. *Chemical Engineering Journal* **2017**, *329*, 220–230. https://doi.org/10.1016/j.cej.2017.05.017.

(144) Jóźwiak, B.; Greer, H. F.; Dzido, G.; Kolanowska, A.; Jędrysiak, R.; Dziadosz, J.; Dzida, M.; Boncel, S. Effect of Ultrasonication Time on Microstructure, Thermal Conductivity, and Viscosity of Ionanofluids with Originally Ultra-Long Multi-Walled Carbon

Nanotubes. *Ultrasonics Sonochemistry* **2021**, *77*, 105681. https://doi.org/10.1016/j.ultsonch.2021.105681.

(145) Ma, P.-C.; Siddiqui, N. A.; Marom, G.; Kim, J.-K. Dispersion and Functionalization of Carbon Nanotubes for Polymer-Based Nanocomposites: A Review. *Composites Part A: Applied Science and Manufacturing* **2010**, *41* (10), 1345–1367. https://doi.org/10.1016/j.compositesa.2010.07.003.

(146) Cheng, Q.; Debnath, S.; O'Neill, L.; Hedderman, T. G.; Gregan, E.; Byrne, H. J. Systematic Study of the Dispersion of SWNTs in Organic Solvents. *J. Phys. Chem. C* **2010**, *114* (11), 4857–4863. https://doi.org/10.1021/jp911202d.

(147) Johnson, D. W.; Dobson, B. P.; Coleman, K. S. A Manufacturing Perspective on Graphene Dispersions. *Current Opinion in Colloid & Interface Science* **2015**, *20* (5–6), 367–382. https://doi.org/10.1016/j.cocis.2015.11.004.

(148) Kolanowska, A.; Wąsik, P.; Zięba, W.; Terzyk, A. P.; Boncel, S. Selective Carboxylation *versus* Layer-by-Layer Unsheathing of Multi-Walled Carbon Nanotubes: New Insights from the Reaction with Boiling Nitrating Mixture. *RSC Adv.* **2019**, *9* (64), 37608–37613. https://doi.org/10.1039/C9RA08300F.

(149) Slobodian, P.; Riha, P.; Olejnik, R.; Cvelbar, U.; Saha, P. Enhancing Effect of KMnO4 Oxidation of Carbon Nanotubes Network Embedded in Elastic Polyurethane on Overall Electro-Mechanical Properties of Composite. *Composites Science and Technology* **2013**, *81*, 54–60. https://doi.org/10.1016/j.compscitech.2013.03.023.

(150) Al Mgheer, T.; H Abdulrazzak, F. Oxidation of Multi-Walled Carbon Nanotubes in Acidic and Basic Piranha Mixture. *Front Nanosci Nanotech* **2016**, *2* (4). https://doi.org/10.15761/FNN.1000127.

(151) Yao, Z.; Wang, C.; Wang, Y.; Qin, J.; Ma, Z.; Cui, X.; Wang, Q.; Wei, H. Effect of CNTs Deposition on Carbon Fiber Followed by Amination on the Interfacial Properties of Epoxy Composites. *Composite Structures* **2022**, *292*, 115665. https://doi.org/10.1016/j.compstruct.2022.115665.

(152) Zabihi, O.; Ahmadi, M.; Akhlaghi Bagherjeri, M.; Naebe, M. One-Pot Synthesis of Aminated Multi-Walled Carbon Nanotube Using Thiol-Ene Click Chemistry for Improvement of Epoxy Nanocomposites Properties. *RSC Adv.* **2015**, *5* (119), 98692–98699. https://doi.org/10.1039/C5RA20338D.

(153) Sohn, G.-J.; Choi, H.-J.; Jeon, I.-Y.; Chang, D. W.; Dai, L.; Baek, J.-B. Water-Dispersible, Sulfonated Hyperbranched Poly(Ether-Ketone) Grafted Multiwalled Carbon

Nanotubes as Oxygen Reduction Catalysts. *ACS Nano* **2012**, *6* (7), 6345–6355. https://doi.org/10.1021/nn301863d.

(154) Samanta, S. K.; Fritsch, M.; Scherf, U.; Gomulya, W.; Bisri, S. Z.; Loi, M. A. Conjugated Polymer-Assisted Dispersion of Single-Wall Carbon Nanotubes: The Power of Polymer Wrapping. *Acc. Chem. Res.* **2014**, *47* (8), 2446–2456. https://doi.org/10.1021/ar500141j.

(155) Kolanowska, A.; Kuziel, A. W.; Herman, A. P.; Jędrysiak, R. G.; Giżewski, T.; Boncel, S. Electroconductive Textile Coatings from Pastes Based on Individualized Multi-Wall Carbon Nanotubes – Synergy of Surfactant and Nanotube Aspect Ratio. *Progress in Organic Coatings* **2019**, *130*, 260–269. https://doi.org/10.1016/j.porgcoat.2019.01.042.

(156) Zhang, Y.; Newton, B.; Lewis, E.; Fu, P. P.; Kafoury, R.; Ray, P. C.; Yu, H. Cytotoxicity of Organic Surface Coating Agents Used for Nanoparticles Synthesis and Stability. *Toxicology in Vitro* **2015**, *29* (4), 762–768. https://doi.org/10.1016/j.tiv.2015.01.017.

(157) Garcia, R. Interfacial Liquid Water on Graphite, Graphene, and 2D Materials. *ACS Nano* **2023**, *17* (1), 51–69. https://doi.org/10.1021/acsnano.2c10215.

(158) Zhou, H.; Ganesh, P.; Presser, V.; Wander, M. C. F.; Fenter, P.; Kent, P. R. C.; Jiang, D.; Chialvo, A. A.; McDonough, J.; Shuford, K. L.; Gogotsi, Y. Understanding Controls on Interfacial Wetting at Epitaxial Graphene: Experiment and Theory. *Phys. Rev. B* **2012**, *85* (3), 035406. https://doi.org/10.1103/PhysRevB.85.035406.

(159) Kim, D.; Kim, E.; Park, S.; Kim, S.; Min, B. K.; Yoon, H. J.; Kwak, K.; Cho, M. Wettability of Graphene and Interfacial Water Structure. *Chem* **2021**, *7* (6), 1602–1614. https://doi.org/10.1016/j.chempr.2021.03.006.

(160) Large, M. J.; Ogilvie, S. P.; Meloni, M.; Amorim Graf, A.; Fratta, G.; Salvage, J.; King, A. A. K.; Dalton, A. B. Functional Liquid Structures by Emulsification of Graphene and Other Two-Dimensional Nanomaterials. *Nanoscale* **2018**, *10* (4), 1582–1586. https://doi.org/10.1039/C7NR05568D.

(161) Chen, Y.; Szkopek, T.; Cerruti, M. Functional Porous Graphene Materials by Pickering Emulsion Templating: From Emulsion Stabilization to Structural Design and Fabrication. *Advances in Colloid and Interface Science* **2025**, *342*, 103536. https://doi.org/10.1016/j.cis.2025.103536.

(162) Festinger, N.; Kisielewska, A.; Burnat, B.; Ranoszek-Soliwoda, K.; Grobelny, J.; Koszelska, K.; Guziejewski, D.; Smarzewska, S. The Influence of Graphene Oxide Composition on Properties of Surface-Modified Metal Electrodes. *Materials* **2022**, *15* (21), 7684. https://doi.org/10.3390/ma15217684.

(163) Najafi, M.; Zahid, M.; Ceseracciu, L.; Safarpour, M.; Athanassiou, A.; Bayer, I. S. Polylactic Acid-Graphene Emulsion Ink Based Conductive Cotton Fabrics. *Journal of Materials Research and Technology* **2022**, *18*, 5197–5211. https://doi.org/10.1016/j.jmrt.2022.04.119.

(164) Mates, J. E.; Bayer, I. S.; Salerno, M.; Carroll, P. J.; Jiang, Z.; Liu, L.; Megaridis, C. M. Durable and Flexible Graphene Composites Based on Artists' Paint for Conductive Paper Applications. *Carbon* **2015**, *87*, 163–174. https://doi.org/10.1016/j.carbon.2015.01.056.

(165) Liu, M.; Zhu, W.; Wang, H. Materials Prepared via Pickering Emulsions Stabilized by Graphene Oxide: Overview and Prospects. *Materials* **2025**, *18* (20), 4790. https://doi.org/10.3390/ma18204790.

(166) Kuziel, A. W.; Milowska, K. Z.; Chau, P.; Boncel, S.; Koziol, K. K.; Yahya, N.; Payne, M. C. The True Amphipathic Nature of Graphene Flakes: A Versatile 2D Stabilizer. *Advanced Materials* **2020**, *32* (34), 2000608. https://doi.org/10.1002/adma.202000608.

(167) Woltornist, S. J.; Oyer, A. J.; Carrillo, J.-M. Y.; Dobrynin, A. V.; Adamson, D. H. Conductive Thin Films of Pristine Graphene by Solvent Interface Trapping. *ACS Nano* **2013**, *7* (8), 7062–7066. https://doi.org/10.1021/nn402371c.

(168) Wang, H.; Hobbie, E. K. Amphiphobic Carbon Nanotubes as Macroemulsion Surfactants. *Langmuir* **2003**, *19* (8), 3091–3093. https://doi.org/10.1021/la026883k.

(169) Briggs, N. M.; Weston, J. S.; Li, B.; Venkataramani, D.; Aichele, C. P.; Harwell, J. H.; Crossley, S. P. Multiwalled Carbon Nanotubes at the Interface of Pickering Emulsions. *Langmuir* **2015**, *31* (48), 13077–13084. https://doi.org/10.1021/acs.langmuir.5b03189.

(170) Shen, M.; Resasco, D. E. Emulsions Stabilized by Carbon Nanotube−Silica Nanohybrids. *Langmuir* **2009**, *25* (18), 10843–10851. https://doi.org/10.1021/la901380b.

(171) Chen, W.; Liu, X.; Liu, Y.; Kim, H.-I. Novel Synthesis of Self-Assembled CNT Microcapsules by O/W Pickering Emulsions. *Materials Letters* **2010**, *64* (23), 2589–2592. https://doi.org/10.1016/j.matlet.2010.08.052.

(172) Blacha, A. W.; Milowska, K. Z.; Payne, M. C.; Greer, H. F.; Terzyk, A. P.; Korczeniewski, E.; Cyganiuk, A.; Boncel, S. The Origin of Amphipathic Nature of Short and Thin Pristine Carbon Nanotubes—Fully Recyclable 1D Water-in-Oil Emulsion Stabilizers. *Adv Materials Inter* **2023**, *10* (7), 2202407. https://doi.org/10.1002/admi.202202407.

(173) Kuziel, A. W.; Dzido, G.; Turczyn, R.; Jędrysiak, R. G.; Kolanowska, A.; Tracz, A.; Zięba, W.; Cyganiuk, A.; Terzyk, A. P.; Boncel, S. Ultra-Long Carbon Nanotube-Paraffin Composites of Record Thermal Conductivity and High Phase Change Enthalpy among

Paraffin-Based Heat Storage Materials. *Journal of Energy Storage* **2021**, *36*, 102396. https://doi.org/10.1016/j.est.2021.102396.

(174) Paredes, J. I.; Villar-Rodil, S. Biomolecule-Assisted Exfoliation and Dispersion of Graphene and Other Two-Dimensional Materials: A Review of Recent Progress and Applications. *Nanoscale* **2016**, *8* (34), 15389–15413. https://doi.org/10.1039/C6NR02039A.

(175) Silverman, H. G.; Roberto, F. F. Understanding Marine Mussel Adhesion. *Mar Biotechnol* **2007**, *9* (6), 661–681. https://doi.org/10.1007/s10126-007-9053-x.

(176) Kuziel, A.; Dzido, G.; Jędrysiak, R. G.; Kolanowska, A.; Jóźwiak, B.; Beunat, J.; Korczeniewski, E.; Zięba, M.; Terzyk, A. P.; Yahya, N.; Thakur, V. K.; Koziol, K. K.; Boncel, S. Biomimetically Inspired Highly Homogeneous Hydrophilization of Graphene with Poly(L -DOPA): Toward Electroconductive Coatings from Water-Processable Paints. *ACS Sustainable Chem. Eng.* **2022**, *10* (20), 6596–6608. https://doi.org/10.1021/acssuschemeng.2c00226.

(177) Herman, A. P.; Boncel, S. Oxidised Carbon Nanotubes as Dual-Domain Synergetic Stabilizers in Electroconductive Carbon Nanotube Flexible Coatings. *RSC Adv.* **2018**, *8* (54), 30712–30716. https://doi.org/10.1039/C8RA05902K.

(178) Xu, H.; Wang, J.; Yang, X.; Ning, L. Magnetically Recyclable Graphene Oxide Demulsifier Adapting Wide pH Conditions on Detachment of Oil in the Crude Oil-in-Water Emulsion. *ACS Appl. Mater. Interfaces* **2021**, *13* (5), 6748–6757. https://doi.org/10.1021/acsami.0c18115.

(179) Wang, X.; Yu, K.; An, R.; Han, L.; Zhang, Y.; Shi, L.; Ran, R. Self-Assembling GO/Modified HEC Hybrid Stabilized Pickering Emulsions and Template Polymerization for Biomedical Hydrogels. *Carbohydrate Polymers* **2019**, *207*, 694–703. https://doi.org/10.1016/j.carbpol.2018.12.034.

(180) Zhang, L.; Wu, K.; Chen, Y.; Liu, R.; Luo, J. The Preparation of Linseed Oil Loaded Graphene/Polyaniline Microcapsule via Emulsion Template Method for Self-Healing Anticorrosion Coatings. *Colloids and Surfaces A: Physicochemical and Engineering Aspects* **2022**, *651*, 129771. https://doi.org/10.1016/j.colsurfa.2022.129771.

(181) Liu, M.; Zhu, W.; Wang, H. Materials Prepared via Pickering Emulsions Stabilized by Graphene Oxide: Overview and Prospects. *Materials* **2025**, *18* (20), 4790. https://doi.org/10.3390/ma18204790.

(182) Necolau, M.-I.; Pandele, A.-M. Recent Advances in Graphene Oxide-Based Anticorrosive Coatings: An Overview. *Coatings* **2020**, *10* (12), 1149. https://doi.org/10.3390/coatings10121149.

(183) Gou, Y.; Han, J.; Li, Y.; Qin, Y.; Li, Q.; Zhong, X. Research on Anti-Icing Performance of Graphene Photothermal Superhydrophobic Surface for Wind Turbine Blades. *Energies* **2022**, *16* (1), 408. https://doi.org/10.3390/en16010408.

(184) Zhang, J.; Kong, G.; Li, S.; Le, Y.; Che, C.; Zhang, S.; Lai, D.; Liao, X. Graphene-Reinforced Epoxy Powder Coating to Achieve High Performance Wear and Corrosion Resistance. *Journal of Materials Research and Technology* **2022**, *20*, 4148–4160. https://doi.org/10.1016/j.jmrt.2022.08.156.

ACADEMIC ACHIEVEMENTS

Publications

1. **[P1] Kuziel A. W.;** , Milowska*, K. Z.; Chau, P.; Boncel, S.; Koziol*, K. K.; Yahya, N.; Payne, M. C.; The true amphipathic nature of graphene flakes: a versatile 2D stabilizer, *Advanced Materials* **2020**, *32*, 2000608; https://doi.org/10.1002/adma.202000608.
2. **[P2] Blacha**, A. W.; Milowska*, K. Z.; Payne, M. C.; Greer, H. F.; Terzyk, A. P.; Korczeniewski, E.; Cyganiuk, A.; Boncel*, S. The Origin of Amphipathic Nature of Short and Thin Pristine Carbon Nanotubes — Fully Recyclable 1D Water-in-Oil Emulsion Stabilizers, *Advanced Materials Interfaces* **2023**, *10*, 2202407; https://doi.org/10.1002/admi.202202407.
3. **[P3] Kuziel**, A. W.; Dzido, G.; Turczyn, R.; Jędrysiak, R. G.; Kolanowska, A.; Tracz, A.; Zięba, W.; Cyganiuk, A.; Terzyk, A. P.; Boncel*; S. Ultra-long carbon nanotube-paraffin composites of record thermal conductivity and high phase change enthalpy among paraffin-based heat storage materials, *Journal of Energy Storage* **2021**, *36,* 102396; https://doi.org/10.1016/j.est.2021.102396.
4. **[P4] Blacha, A.;** Dzido, G.; Jędrysiak, R.; Kolanowska, A.; Jóźwiak, B.; Beunat, J.; Korczeniewski, E.; Zięba, M.; Terzic, A. P.; Yahya, N.; Thakur, V. K.; Kozioł*, K. K.; Boncel*, S. Biomimetically inspired highly homogeneous hydrophilization of graphene with poly(L-DOPA): toward electroconductive coatings from water-processable paints, *ACS Sustainable Chemistry Engineering* **2022,** *10*(20), 6596–6608; https://doi.org/10.1021/acssuschemeng.2c00226.
5. Jóźwiak, B.; Scheller, Ł.; Greer, H. F.; Cwynar, K.; Urbaniec, K.; Dzido, G.; Dziadosz, J.; Jędrysiak, R.; Kolanowska, A.; **Blacha, A**.; Boncel, S.; Dzida, M. Water-like Thermal Conductivity of Ionanofluids Containing High Aspect Ratio Multi-Walled Carbon Nanotubes and 1-Ethyl-3-Methylimidazolium-Based Ionic Liquids with Cyano-

Functionalized Anions. *Journal of Molecular Liquids* **2023**, *391*, 123329. https://doi.org/10.1016/j.molliq.2023.123329.

6. Boncel, S.; Jędrysiak, R. G.; Czerw, M.; Kolanowska, A.; **Blacha, A**. W.; Imielski, M.; Jóźwiak, B.; Dzida, M. H.; Greer, H. F.; Sobotnicki, A. Paintable Carbon Nanotube Coating-Based Textronics for Sustained Holter-Type Electrocardiography. *ACS Appl. Nano Mater.* **2022**, *5* (10), 15762–15774. https://doi.org/10.1021/acsanm.2c03904.
7. Dzida, M.; Boncel, S.; Jóźwiak, B.; Greer, H. F.; Dulski, M.; Scheller, Ł.; Golba, A.; Flamholc, R.; Dzido, G.; Dziadosz, J.; Kolanowska, A.; Jędrysiak, R.; **Blacha, A.;** Cwynar, K.; Zorębski, E.; Bernardes, C. E. S.; Lourenço, M. J. V.; Nieto De Castro, C. A. High-Performance Ionanofluids from Subzipped Carbon Nanotube Networks. *ACS Appl. Mater. Interfaces* **2022**, *14* (45), 50836–50848. https://doi.org/10.1021/acsami.2c14057.
8. Górski, M.; Czulkin, P.; Wielgus, N.; Boncel, S.; **Kuziel, A**. W.; Kolanowska, A.; Jędrysiak, R. G. Electrical Properties of the Carbon Nanotube-Reinforced Geopolymer Studied by Impedance Spectroscopy. *Materials* **2022**, *15* (10), 3543. https://doi.org/10.3390/ma15103543.
9. Traciak, J.; Koziol, K.; Małecka, M.; **Blacha, A**.; Boncel, S.; Żyła, G. The First Step into Material Table Dataset for Surface Tension of Nanofluids: Insights from the Case Study of Ethylene Glycol-Based Graphene Nanofluids. *Int J Thermophys* **2025**, *46* (7), 93. https://doi.org/10.1007/s10765-025-03553-1.
10. Kolanowska, A.; **Kuziel, A**. W.; Herman, A. P.; Jędrysiak, R. G.; Giżewski, T.; Boncel, S. Electroconductive Textile Coatings from Pastes Based on Individualized Multi-Wall Carbon Nanotubes – Synergy of Surfactant and Nanotube Aspect Ratio. *Progress in Organic Coatings* **2019**, *130*, 260–269. https://doi.org/10.1016/j.porgcoat.2019.01.042.
11. Kolanowska, A.; **Kuziel, A.** W.; Jędrysiak, R. G.; Krzywiecki, M.; Korczeniewski, E.; Wiśniewski, M.; Terzyk, A. P.; Boncel, S. Ullmann Reactions of Carbon Nanotubes—

Advantageous and Unexplored Functionalization toward Tunable Surface Chemistry. *Nanomaterials* **2019**, *9* (11), 1619. https://doi.org/10.3390/nano9111619.

12. Boncel, S.; Kolanowska, A.; **Kuziel, A**. W.; Krzyżewska, I. Carbon Nanotube Wind Turbine Blades: How Far Are We Today from Laboratory Tests to Industrial Implementation? *ACS Appl. Nano Mater.* **2018**, *1* (12), 6542–6555. https://doi.org/10.1021/acsanm.8b01824.
13. Kolanowska, A.; **Kuziel, A**.; Li, Y.; Jurczyk, S.; Boncel, S. Rieche Formylation of Carbon Nanotubes – One-Step and Versatile Functionalization Route. *RSC Adv.* **2017**, *7* (81), 51374–51381. https://doi.org/10.1039/C7RA10525H.

Projects

1. Project NCN OPUS-20 UMO-2020/39/B/ST5/02562 pt. „IoNanoFluids – 'ionic liquid-nanocarbon' hybrids as superlubricants in metal-polymer friction pairs" (04.2025 – 10.2025), role: stipendist
2. Project NCN OPUS-17 UMO-2019/33/B/ST5/01412 pt. „Individualization and 'networking' of carbon nanotubes – interdependent chemical modifications in the quest for novel nanomaterials", (11.2020-05.2024); role: stipendist
3. Project NCN OPUS-14 UMO-2017/27/B/ST4/02748 pt. „Synthesis, stability, structure and physicochemical properties of ionic liquids with carbon nanostructures as energy storage materials", (10.2018-04.2023), role: stipendist
4. Project NCBiR TANGO-1 TANGO1/266702/NCBR/2016 pt. „The impact of chemical modification of carbon nanostructures on the electromagnetic properties of composites and hybrid materials", (12.2016 – 06.2018), role: stipendist.
5. Project MNiSW: Najlepsi z najlepszych! 4.0.: Functional carbon nanomaterials – from synthesis via chemical modifications to ready-to-use products, (07.2019 – 06.2020), role: stipendist

Own projects related to status research (PL: 'badania statutowe')

1. Project BKM: Modyfikacja chemiczna powłok termo- i elektroprzewodzących zawierających nanorurki węglowe, (04.2024 – 12.2024).
2. Project BKM: Otrzymywanie powłok termo- i elektroprzewodzących zawierających nanorurki węglowe i grafen, (04.2022 – 12.2022).
3. Project BKM: Tethering macromolecules: the art of making graphene hydrophilic and amphiphilic, (04.2021 – 12.2021).

Internship

1. 08.2021-09.2021, ENS Paris-Saclay University, France,

   Theme: Synthesis and characterisation of *s*-tetrazine functionalized CNTs.
2. 06.2018-09.2018, Cranfield University and Cambridge University, UK.

   Theme: synthesis and characterisation of hybrid graphene structures

Conferences

1. 9th Internanotional Conference InterNanoPoland 2025, 8-9.10.2025, Katowice, Polska: Carbon Nanomaterials at the Oil-Water Interphases: Pathways to Greener Emulsion Stabilization (poster).
2. X Międzynarodowa Interdyscyplinarna Konferencja Doktorantów Uczelni Technicznych – InterTechDoc'2025;15-17.09.2024, Zabrze, Polska; Amphipathic Graphene Flakes and Carbon Nanotubes: New Frontiers in Sustainable Emulsion Stabilization (poster).
3. 8th International Conference InterNanoPoland 2024, 16-17.10.2024, Katowice, Polska; Cross-linking of carbon nanotubes using *s*-tetrazine derivatives (poster).
4. NT24: The 24th International Conference on Science and Application of Nanotubes and Low-Dimensional Materials, 23-28.06.2024 Boston, Cambridge, USA; Cross-linking of carbon nanotubes using *s*-tetrazine derivatives (poster).

5. 64. Zjazd Naukowy PTChem, 11-16.09. 2022, Lublin, Polska; Sieciowanie nanorurek węglowych za pomocą pochodnych s-tetrazyn (poster).
6. XV Kopernikańskie Seminarium Doktoranckie, 20-22.06.2022, Toruń, Polska; Otrzymywanie powłok elektroprzewodzących zawierających modyfikowane nanorurki węglowe (poster).
7. VI Międzynarodowa Interdyscyplinarna Konferencja Doktorantów Uczelni Technicznych – InterTechDoc'2021, 21-23.07.2021, Ustroń, Polska; Metody otrzymywania hydrofilowego grafenu (komunikat ustny).
8. 6th NANO Boston Conference, 07-09.2020, Boston, Cambridge, USA; Roofing with integrated heating coating based on nanocarbon structures (poster).
9. 2nd Global Conference on Carbon Nanotubes and Graphene Technologies, 13-14.02.2020, Lizbona, Portugalia; Ullman-type Reactions of Carbon Nanotubes – Novel Route in Chemistry of sp^2-carbon (poster).
10. NT19: 20th International Conference on the Science and Application of Nanotubes and Low-Dimensional Materials: 21-26.07.2019, Würzburg, Niemcy; Synthesis and Thermal Properties of Helical CNTs Ionic Liquid Nanofludis (poster).
11. 8th European Young Engineers Conference, 8-10.04.2019, Warsaw, Poland;
    a) c-CVD synthesis of helical carbon nanotubes as potential energy storage nanomaterials (poster)
    b) The impact of purification and characteristics of carbon nanotubes onto their dispersibility in ionic liquids (poster).
12. 2nd International Conference on Graphene commercialization: from product to prototypes, 19.09.2018; Crnafield, UK;
    a) Conductive graphene coatings (poster),
    b) Polystyrene grafted graphene structures (komunikat ustny),

c) Organic solvent as a surfactant in dispersing of graphene in water (poster).

13. 7th European Young Engineers Conference, 23-25.04.2018, Warsaw, Poland; From low-molecular weight analogues to carbon nanotubes- chemistry of azides towards functionalization of sp^2-nanocarbons (poster).
14. Wiosenny Zjazd Sekcji Studenckiej PTChem, 25-29.04.2018, Skorzęcin, Polska;The solvent effect in the Ullmann reaction of chlorinated carbon nanotubes (poster).
15. 2nd International Conference InterNanoPoland 2017, 22-23.06.2017, Katowice, Polska;
    a) Formylation of carbon nanotubes (poster),
    b) Electroconductive paths printable from carbon nanotube paint (poster).

Achievements

1. The START Scholarship awarded by the Foundation for Polish Science in 2025 for outstanding young researchers at the beginning of their scientific careers.
2. Poster Award from RSC Materials Horizons at the InterNanoPoland 2024 conference.
3. 2nd place in the competition for the best scientific poster presented during the 15th Copernican Doctoral Seminar (June 20–22, 2022, Toruń).
4. Rector's Scholarship of the Silesian University of Technology for the best PhD students fo academic year 2020/2021.
5. Scholarship of the Minister of Science and Higher Education for outstanding scientific achievements for academic years 2018/2019 and 2019/2020.
6. Jan Binkiewicz Scholarship for outstanding students for the academic year 2018/2019.
7. Special distinction by DuPont in the national competition Golden Medal of Chemistry 2019 for the best engineering thesis completed in the academic year 2018/2019.
8. Poster award at the InterNanoPoland 2017 conference.

Other activities

1. Scientific supervisor of the Student Scientific Circle of Chemists at the Silesian University of Technology.
2. Assistant supervisor in two research projects conducted with high schools as part of the *"Politechnika Project"*:

   a) Preparation of electroconductive pastes containing carbon nanotubes;

   b) Preparation of electro- and thermoconductive films containing modified carbon nanotubes.
3. Member of the University Council of Doctoral Students at the Silesian University of Technology during the 2021/2022 and 2022/2023 terms.

AUTHOR'S CONTRIBUTION

Publication P1 (35%)

- Preparation of the literature review
- Performance of all the wet chemistry experiments
- Characterisation of the materials
- Performing the optical microscopy and SEM images
- Analysis of the obtained results
- Preparation of the manuscript drafts and graphics
- Contribution to manuscript editing and preparation of responses to reviewers.

Publication P2 (35%)

- Preparation of the literature review
- Performance of all the wet chemistry experiments
- Characterisation of the materials and emulsions (Optical images, Raman spectroscopy, TGA, titration)
- Preparation of the paints and characterisation of the coatings
- Analysis of the obtained results
- Preparation of the manuscript drafts and graphics
- Contribution to manuscript editing and preparation of responses to reviewers.

Publication P3 (45%)

- Preparation of the literature review
- Performance of all the wet chemistry experiments
- Performing the optical microscopy
- Analysis of the obtained results (SEM, TEM, TGA, XRD, Raman Spectroscopy, DSC, thermal conductivity)

- Preparation of the manuscript drafts and graphics
- Contribution to manuscript editing and preparation of responses to reviewers.

Publication P4 (35%)

- Preparation of the literature review
- Performance the wet chemistry experiments
- Performing the optical microscopy, elemental analysis, FTIR, Raman spectroscopy, titration, ESI-MS;
- Preparation of the paints, coating and electrical and mechanical characterisation
- Analysis of the obtained results
- Preparation of the manuscript drafts
- Contribution to manuscript editing and preparation of responses to reviewers.